Journal of Medicinal Chemistry

Article

Structural optimization and pharmacological evaluation of inhibitors targeting dual-specificity tyrosine phosphorylation-regulated kinases (DYRK) and CDC-like kinases (CLK) in glioblastoma

Qing-Qing Zhou, Athena F. Phoa, Ramzi H. Abbassi, Monira Hoque, Tristan A. Reekie, Josep S. Font, Renae M. Ryan, Brett W. Stringer, Bryan W. Day, Terrance G Johns, Lenka Munoz, and Michael Kassiou

J. Med. Chem., **Just Accepted Manuscript** • DOI: 10.1021/acs.jmedchem.6b01840 • Publication Date (Web): 16 Feb 2017

ACS Publications

Journal of Medicinal Chemistry is published by the American Chemical Society. 1155 Sixteenth Street N.W., Washington, DC 20036

Structural optimization and pharmacological evaluation of inhibitors targeting dual-specificity tyrosine phosphorylation-regulated kinases (DYRK) and CDC-like kinases (CLK) in glioblastoma

Qingqing Zhou[1], Athena F. Phoa[2], Ramzi H. Abbassi[2], Monira Hoque[2], Tristan A. Reekie[1], Josep S. Font[3], Renae M. Ryan[3], Brett W. Stringer[4], Bryan W. Day[4], Terrance G. Johns[5], Lenka Munoz[2*] and Michael Kassiou[1*]

[1]*School of Chemistry, The University of Sydney, New South Wales 2006, Australia*

[2]*School of Medical Sciences, Discipline of Pathology and Charles Perkins Centre, The University of Sydney, New South Wales 2006, Australia*

[3]*School of Medical Sciences, Discipline of Pharmacology, The University of Sydney, New South Wales 2006, Australia*

[4]*QIMR Berghofer Medical Research Institute, 300 Herston Road, Herston, Queensland 4006, Australia*

[5]*Oncogenic Signaling Laboratory, Centre for Cancer Research, Hudson Institute of Medical Research, 27 Wright Street, Clayton, Victoria 3168, Australia*

ABSTRACT (150 words)

The DYRK family contains kinases that are up-regulated in malignancy and control several cancer hallmarks. To assess the anti-cancer potential of inhibitors targeting DYRK kinases, we developed a series of novel DYRK inhibitors based on the 7-azaindole scaffold. All compounds were tested for their ability to inhibit DYRK1A, DYRK1B, DYRK2 and the structurally related CLK1. The library was screened for anti-cancer efficacy in established and stem cell-like glioblastoma cell lines. The most potent inhibitors ($IC_{50} \leq 50$ nM) significantly decreased viability, clonogenic survival, migration and invasion of glioblastoma cells. Target engagement was confirmed with genetic knockdown and the cellular thermal shift assay. We demonstrate that DYRK1A's thermal stability in cells is increased upon compound treatment, confirming binding in cells. In summary, we present synthesis, structure-activity relationship and efficacy in glioblastoma-relevant models for a library of novel 7-azaindoles.

INTRODUCTION

Dual-specificity tyrosine phosphorylation-regulated kinases (DYRK) and CDC-like kinases (CLKs) are members of the CMGC group of proline-directed kinases, which also includes cyclin-dependent kinases (CDKs), mitogen-activated protein kinases (MAPKs) and glycogen synthase kinases (GSKs).[1, 2] While the CDK, GSK and MAPK signaling pathways have been extensively studied with numerous inhibitors developed; less in known about DYRK and CLK signaling with the development of inhibitors only becoming of interest recently.

The DYRK family consist of 5 kinases (DYRK1A, DYRK1B, DYRK2, DYRK3, DYRK4) with DYRK1A being the most studied subtype. DYRK1A is produced as a constitutively active kinase and its activity is controlled by subtle changes in the expression levels, in contrast to the more paradigmatic phosphorylation-regulated activation of MAPKs, CDKs and CLKs. Increased DYRK1A expression induces phosphorylation of substrates at serine/threonine residues which modulates various pathological processes.[3, 4] Most notably, the *DYRK1A* gene maps to chromosome 21 and the extra gene copy in Down syndrome individuals results in 1.5-fold increased DYRK1A expression. This alteration in DYRK1A expression levels has been correlated with structural changes and cognitive impairment in Down syndrome population.[5] Furthermore, trisomy 21-mediated DYRK1A up-regulation has been linked to increased risk of childhood leukaemia and early onset of Alzheimer's disease.[6]

Potent ATP-competitive DYRK1A inhibitors have emerged from natural sources, such as meridianines,[7] leucettine L41[8] and the alkaloid harmine (**1**; Figure 1), which is the most experimentally used DYRK1A inhibitor. This small β-carboline alkaloid (**1**) inhibits DYRK1A (IC_{50} = 33-80 nM) [9-11] and other kinases of the DYRK family; IC_{50} values of 0.16 μM (DYRK1B), 2 μM (DYRK2), 0.41 μM (DYRK3) and 80 μM (DYRK4) have been reported [9, 10]. From a series of analogues of the marine sponge leucettine, leucettine L41 with potent inhibition of DYRK1A (IC_{50} = 55 nM) and CLK1 (IC_{50} = 71 nM) was developed.

Heterocyclic DYRK1A inhibitors not derived from natural products are represented by the benzothiazole (INDY) (**2a**)[12] and 7-azaindole (DANDY) (**3a**)[13] (Figure 1). **2a** is a derivative of the CLK inhibitor TG003 (**2b**)[14, 15] that inhibits DYRK1A with IC_{50} = 240 nM, although is equipotent at inhibiting other DYRK and CLK subtypes. The **3a**-type inhibitors remain one of the most potent DYRK1A inhibitors to date. The lead molecules in this series inhibit DYRK1A and CLK1 at low nanomolar concentrations (IC_{50} = 3 - 20 nM).[12, 13] As all DYRK1A inhibitors inhibit related kinases of the CMGC group (e.g. DYRK1B, DYRK2, CLK1, CLK4, CDK5), efforts have been directed towards the development of selective DYRK1A inhibitors.[16, 17] For example, quinolone-6-carboxylic acid based inhibitor resulted in a DYRK1A selective inhibitor which displayed a 100-fold selectivity for DYRK1A (IC_{50} = 6 nM) over DYRK1B (IC_{50} = 600 nM) and CLK1 (IC_{50} = 500 nM).[17] More recent efforts developed quinazoline-2-carbimidates selective for DYRK1A and DYRK1B.[18] Selective inhibitors are valuable tools to probe DYRK1A pathways and could serve as leads for the development of new drugs to ameliorate the cognitive deficits in the population affected by Down syndrome.

Cancer, however, is a complex disease driven by deregulation of numerous pathways and molecularly targeted cancer therapy has greatly benefited from kinase inhibitors targeting multiple kinases. Increasing evidence suggests that DYRK and CLK kinases are over-expressed in tumours[19-21] where they have been linked to the deregulation of cell cycle through various mechanisms.[22-24,25, 26] For example, DYRK1A-dependent phosphorylation of Sprouty2 blocks degradation of the epidermal growth factor receptor (EGFR)[27, 28-29, 30] and favors recycling of EGFR to the cell surface to amplify cancer cell proliferation. Furthermore, DYRK1A and CLK1 are prime regulators of alternative splicing. Through this mechanism, DYRK1A and CLK1 not only increase cell proliferation,[31] but also increase expression of anti-apoptotic proteins Bcl-X_L and Mcl-1[32], resulting in resistance to apoptotic stimuli. DYRK1B induce reversible cell arrest in a quiescent state and inhibition of DYRK1B has been suggested to renew the cell cycle and sensitize cancer cells to chemotherapy and molecularly targeted therapy.[25, 33-36] Finally, DYRK kinases

phosphorylate actin and tubulin, which are cytoskeletal proteins crucial for cell migration.[37-39] Thus, inhibition of this kinase family might be a beneficial strategy to combat proliferation and migration of cancer cells.

Herein, we describe the synthesis of novel 7-azaindole based inhibitors and pharmacological evaluation against DYRK1A, DYRK1B, DYRK2 and CLK1. We extended the structure-activity relationship (SAR) of this series of compounds by employing primarily a bioisosteric approach where we explored substitution of the phenol group at the C3 or C5 position of compound **3a** independently. Furthermore, we have chosen to evaluate these novel inhibitors in a glioblastoma-relevant model as DYRK kinases are over-expressed in glioblastoma tumors and genetic knock-down of DYRK1A reduced tumor growth *in vivo*, suggesting that DYRK inhibitors could have therapeutic potential.

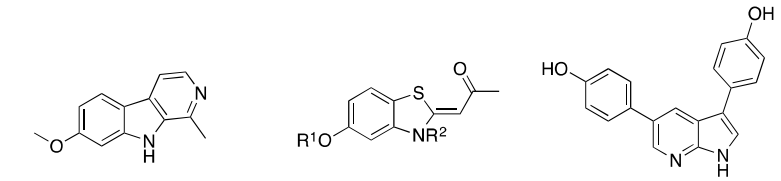

Figure 1. Selected DYRK1A inhibitors

RESULTS AND DISCUSSION

SYNTHESIS

The synthesis of **3a** followed the published method[13] starting from 5-bromo-7-azaindole (**4a**) (**Scheme 1**). Regioselective iodination at the 3-position with *N*-iodosuccinimide afforded **5a** followed by *p*-toluenesulfonyl (tosyl) protection to give **6a**. Suzuki cross-coupling at both halide positions afforded the diaryl compound **7a**, which could then be deprotected, first by removing the tosyl group to give **8a**, followed by demethylation affording the lead compound **3a**. We then generated a library of **3a** analogues. Initial investigations focused on the 7-azaindole core and what changes could be tolerated. The indole and indazole based compounds, **3b** and **3c** respectively, were prepared in an analogous manner to **3a** (**Scheme 1**).

Scheme 1. Synthetic route of diphenol-azaindole derivatives[a]

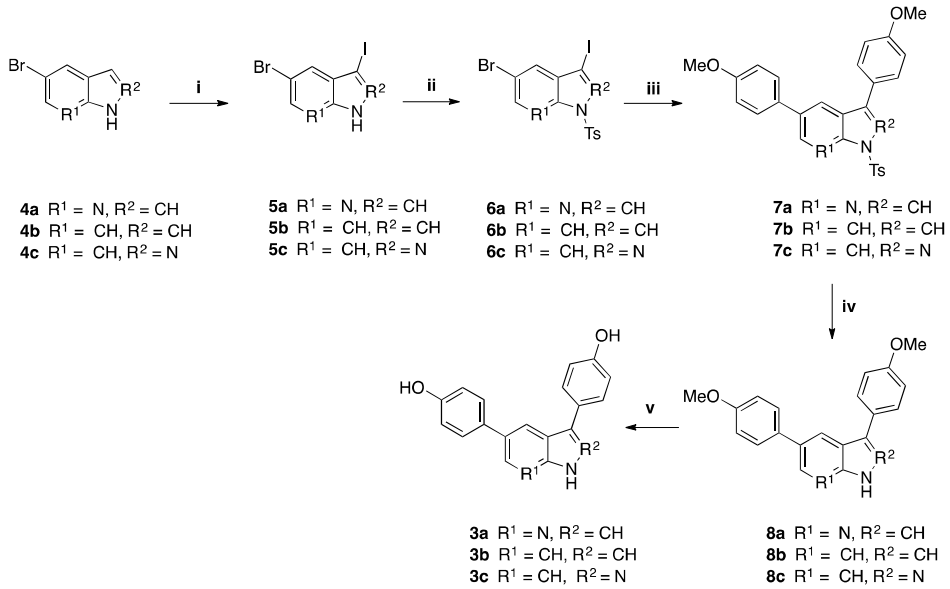

[a]Reagents and conditions: (i) NIS (1.0 eq), KOH (0.5 eq), CH_2Cl_2, RT, 10 h; (ii) NaH (60% in mineral oil, 3.0 eq), TsCl (1.2 eq), $BnEt_3NCl$ (0.02 eq), CH_2Cl_2, 0-RT, 30 min; 80-89% over two steps; (iii) arylboronic acid (2.0 eq), $Pd(PPh_3)_4$ (4 mol%), K_2CO_3 2 M (4.0 eq), toluene/EtOH 3:1, 100 °C, 3.5 h, 84-87%; (iv) KOH (5.0 eq), MeOH, 80 °C, 2 h, 91-95%; (v) BBr_3 (6.0 eq), CH_2Cl_2, 0 °C to RT, 15 h, 58-65%. NIS = *N*-iodosuccinimide.

Next, we focused on the modification of the phenol group at the C3 or C5 position of the azaindole scaffold, utilizing the key intermediate **6a**. Sequential Suzuki cross-coupling reactions[40, 41] were employed to first afford **7d-g**, then the desired diaryl-substituted compounds **8d-i** (**Scheme 2**). Hydrolysis of the tosyl group under basic conditions resulted in compounds **9a-c** and **9e-g**. The desired compounds **8j-k** were realized by cyclization[42] of the benzonitriles **8f** or **8i**, respectively, with $TMSN_3$ under microwave conditions followed by hydrolysis of the tosyl group. The nitro-substituted compounds **9a** and **9e** were reduced in the presence of iron powder under acidic conditions to afford anilines **9d** and **9h**, respectively. Further modifications were performed on the

newly formed aniline **9h** by acetylation[43] or sulfonylamide formation[44] with treatment of acetic anhydride in acetic acid or with methanesulfonyl chloride in H_2O to afford **10a** and **10b**, respectively. The compound **10c** was also obtained in 70% yield from urea and catalyzed by iodine and citric acid in mannitol.[45]

Scheme 2. Synthetic route of aryl-azaindole derivatives[a]

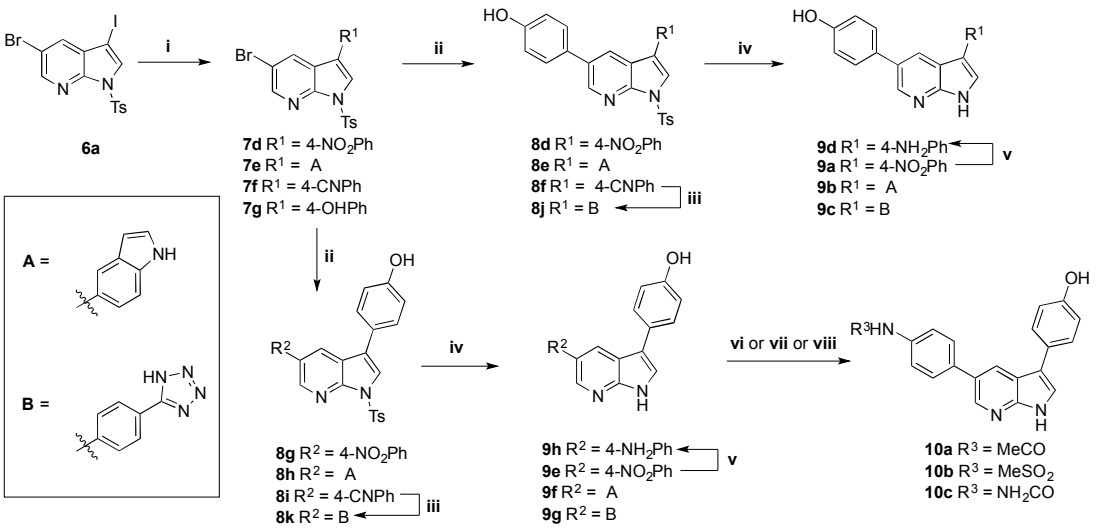

[a]Reagents and conditions: (i) arylboronic acid, $Pd(PPh_3)_4$ (2 mol%), K_2CO_3 2 M (2.0 eq), toluene/EtOH 3:1, 90 °C, 3-5 h, 78-85%; (ii) arylboronic acid, $Pd(PPh_3)_4$ (2 mol%), K_2CO_3 2 M (2.0 eq), toluene/EtOH 3:1, 110 °C, 3-5 h, 80-93%; (iii) TBAF, $TMSN_3$, sodium ascorbate, $CuSO_4$•$5H_2O$, *t*BuOH/H_2O, 1:1 (V/V), MW (100 w, 80 °C), 2 h, 81-83%; (iv) KOH, MeOH, 80 °C, 2 h, 90-95%; (v) Fe powder (10.0 eq), HCl (3 N solution in water, 0.03 M), 110 °C, 3 h, 70-84%; (vi) Ac_2O (1.2 eq), AcOH, 110 °C, 5 h, 77%; (vii) methanesulfonyl chloride (1.5 eq), H_2O, RT, 10 h, 64%; (viii) urea (15.0 eq), I_2 (0.1 eq), citric acid, mannitol, 80 °C, 6 h, 70%.

To investigate diverse skeletons with different geometries and increased spatial flexibility, we added a linker between the 7-aza-indole core and phenol group and varied the phenol substitution resulting in compounds **17a-b** and **21a-b** (Scheme 3). The 5-carboxamide **17a-b** could be easily prepared from **4a**, the same starting material used previously, which was firstly protected with the tosyl group, followed by the formation of the 5-carboxylic acid **12** by palladium-catalyzed carboxylation using freshly made acetic-formic anhydride.[46] The resulting acid underwent HBTU amide coupling with aniline derivative **13a** or **13b** to afford compounds **14a-b** in comparable

yield.[47] Concomitant deprotection of the tosyl and TBS groups gave compounds **15a-b**,[48] which followed by iodination at the C3 position with I_2 and KOH,[49] gave compounds **16a-b**. The final compounds **17a-b** could then be easily obtained by a standard Suzuki cross-coupling reaction. Similarly, compounds **21a-b** could be obtained by again starting with **4a** (Scheme 3), firstly by acylation with trichloroacetyl chloride[50] followed by hydrolysis to afford carboxylic acid **18**. Subsequent amide formation with **13a-b** afforded **19a-b**, which, followed by Suzuki-coupling gave **20a-b**. Final compounds **21a-b** were obtained in high yield after the TBAF induced deprotection of the TBS group.[51]

Scheme 3. Further modification for lead compound **3a**[a]

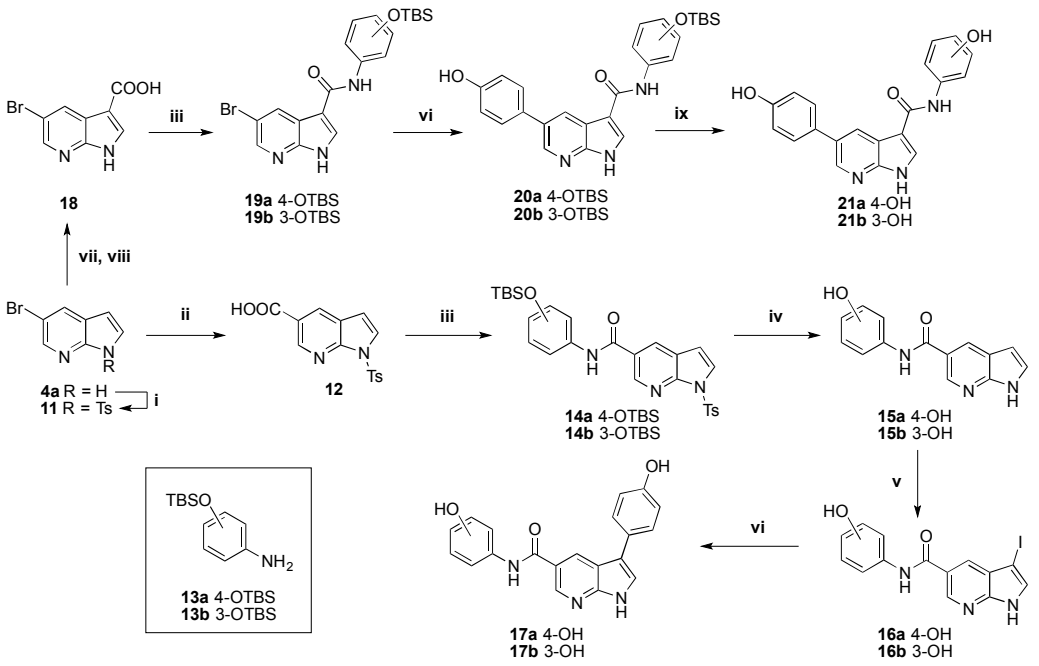

[a]Reagents and conditions: (i) tosyl chloride (1.2 eq), NaH (1.5 eq), THF, 0 °C, 1 h, 90%; (ii) $Pd(OAc)_2$ (5 mol%), dppf (10 mol%), acetic-formic anhydride (5.0 eq), DIPEA (5.0 eq), DMF, 110 °C, 5 h, 83%; (iii) HBTU (1.2 eq), DIPEA (2.5 eq), aniline **13a** or **13b** (1.1 eq), DMSO, 0~RT, 2 h, 61-79%; (iv) KOH (5.0 eq), MeOH, 80 °C, 1 h, 94-96%; (v) I_2 (1.2 eq), KOH (3.0 eq), DMF, RT, 8 h, 80-86%; (vi) arylboronic acid, $Pd(PPh_3)_4$ (2 mol%), K_2CO_3 2 M (2.0 eq), toluene/EtOH 3:1, 100 °C, 3-5 h, 60-65%; (vii) trichloroacetyl chloride (1.2 eq), $AlCl_3$ (2.5 eq), 0 °C, 3 h; (viii) NaOH (3

M), RT, 5 h, 70% over two steps; (ix) TBAF (1.5 eq), THF, RT, 30 min, 93-95%. DIPEA = *N,N*-diisopropylethylamine, dppf =1,1'-ferrocenediyl-bis(diphenylphosphine), HBTU = (2-(1*H*-benzotriazol-1-yl)-1,1,3,3-tetramethyluronium hexafluorophosphate), TBAF = *tetra-n*-butylammonium fluoride, OTBS = *tert*-butyldimethylsilyl ether.

STRUCTURE-ACTVITY RELATIONSHIP

New derivatives were tested for their potency to inhibit DYRK1A, DYRK1B, DYRK2 and CLK1. Kinase assays were performed with Woodtide as a substrate for DYRK kinases and RS peptide as a substrate for CLK1. ATP concentration (100 μM) was kept constant to allow comparison of potencies across the kinases. In our hands, harmine (**1**) and the lead analogue **3a** inhibited DYRK1A with IC_{50} of 360 and 14 nM, respectively. Inhibitor **3a** showed comparable potencies against DYRK1B (15 nM) and CLK1 (48 nM), but it was 10-fold less potent at inhibiting DYRK2 (166 nM, Table 1). Replacement of the azaindole with indole (**3b**) or benzimidazole (**3c)** led to the loss of kinase inhibition (> 1 μM).

Table 1. Kinase inhibition and cellular efficacy of **3a-c** and C3-modified analogues **9b-d**.

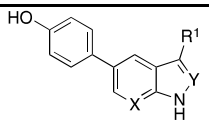

		Kinase inhibition assay (IC_{50}, nM)				Cell viability assay (EC_{50}, μM)			
	X, Y and R^1	***DYRK1A***	***DYRK1B***	***DYRK2***	***CLK1***	***RN1***	***WK1***	***JK2***	***SJH1***
3a	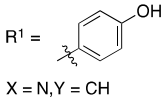 X = N,Y = CH	14 ± 2	15 ± 5	166 ± 22	48 ± 7	2.0 ± 0.4	1.1 ± 0.1	5.1 ± 0.6	4.1 ± 1.0
3b	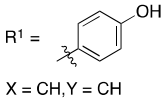 X = CH,Y = CH	>1,000	>1,000	>1,000	>1,000	> 50	> 50	> 50	> 50
3c	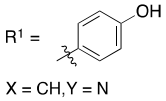 X = CH,Y = N	>1,000	>1,000	>1,000	>1,000	> 50	> 50	> 50	> 50
9b	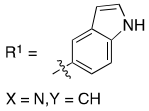 X = N,Y = CH	169 ± 52	83 ± 25	571 ± 149	117 ± 35	5.7 ± 1.3	6.2 ± 2.3	6.3 ± 1.7	2.2 ± 0.5
9c	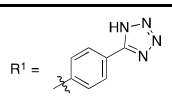 X = N,Y = CH	280 ± 53	172 ± 53	416 ± 46	85 ± 5	> 50	> 50	> 50	> 50

9d	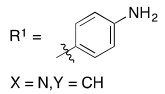	>1,000	>1,000	>1,000	>1,000	> 50	> 50	> 50	> 50

Next, we tested how modification of the phenol at the C3 position affects kinase inhibition. Bioisosteric replacement of the phenol moiety with indole (**9b**) resulted in 10-fold weaker DYRK1A inhibition (169 nM) and comparable loss of activity was observed against DYRK1B (83 nM), DYRK2 (571 nM) and CLK1 (117 nM). Substitution of phenol for a phenyltetrazole moiety at C3 as seen in **9c** further reduced kinase inhibition activity (85 - 280 nM) and the aniline analogue (**9d**) resulted in complete loss of kinase inhibition (> 1 μM).

Based on this SAR, we retained the 7-azaindole core and C3 phenol, but diversified substitution on C5 (Table 2). 4-Nitrophenyl (**9e**) and indole (**9f**) analogues showed weaker DYRK1A inhibition (212 and 204 nM, respectively). Interestingly, indole-analogue **9f** was more potent at inhibiting DYRK1B (51 nM) and CLK1 (26 nM). Analogues with phenyltetrazole (**9g**), aniline (**9h**), sulfonamide (**10b**) or urea (**10c**) in the para-position of the C5 phenyl inhibited DYRK1A with IC_{50} in double-digit nanomolar potency (31 - 86 nM). Comparable nanomolar potency was determined for these inhibitors against DYRK1B and CLK1, and approximately 10-fold higher IC_{50} were calculated from the DYRK2 inhibition assay. The introduction of phenylacetamide at C5 (**10a**) led to the strongest DYRK1A inhibition (6.6 nM) with 5-fold selectivity over DYRK1B (38 nM) and CLK1 (35 nM), and 80-fold selectivity over DYRK2 (536 nM).

Table 2. Kinase inhibition and cellular efficacy of C5 analogues.

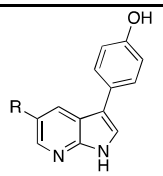

		Kinase inhibition assay (IC_{50}, nM)				Cell viability assay (EC_{50}, µM)			
	R	***DYRK1A***	***DYRK1B***	***DYRK2***	***CLK1***	***RN1***	***WK1***	***JK2***	***SJH1***
9e	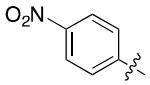	212 ± 36	198 ± 45	>1,000	187 ± 27	> 50	> 50	> 50	> 50
9f	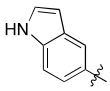	204 ± 46	51 ± 8	644 ± 99	26 ± 6	> 50	> 50	> 50	30 ± 5
9g	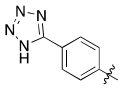	86 ± 17	42 ± 6	408 ± 60	70 ± 9	> 50	> 50	> 50	> 50
9h	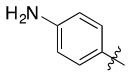	43 ± 9	32 ± 16	567 ± 168	34 ± 8	1.1 ± 0.3	0.9 ± 0.3	8.0 ± 0.2	3.2 ± 0.3
10a	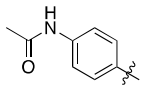	6.6 ± 1.2	38 ± 15	536 ± 108	35 ± 3.5	2.1 ± 0.3	0.9 ± 0.2	8.6 ± 1.7	5.1 ± 0.8
10b	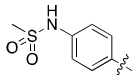	56 ± 17	130 ± 37	724 ± 153	44 ± 14	14 ± 4	42 ± 5	13 ± 2	42 ± 6
10c	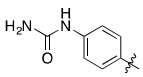	31 ± 10	17 ± 8	476 ± 60	9.6 ± 1.5	22 ± 4	>50	> 50	28 ± 8

Table 3. Kinase inhibition and cellular efficacy of analogues with an amide linker.

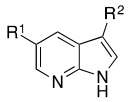

		Kinase inhibition assay (IC_{50}, nM)				Cell viability assay (EC_{50}, µM)			
	R^1 and R^2	*DYRK1A*	*DYRK1B*	*DYRK2*	*CLK1*	*RN1*	*WK1*	*JK2*	*SJH1*
17a	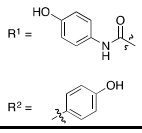	344 ± 84	128 ± 31	>1,000	12 ± 3	12.5 ± 2.9	21.0 ± 4.7	37.8 ± 3.4	5.2 ± 2.2
17b	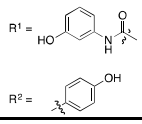	127 ± 54	138 ± 51	847 ± 50	34 ± 8	13.8 ± 1.2	13.2 ± 1.2	38.9 ± 0.1	5.7 ± 0.1
21a	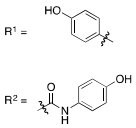	>1,000	>1,000	>1,000	>1,000	> 50	> 50	> 50	> 50
21b	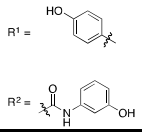	>1,000	>1,000	>1,000	>1,000	> 50	> 50	> 50	> 50

In the final series (Table 3), we explored the effect of an amide linker at position C3 or C5 on kinase inhibition. In line with results obtained with C3 modified analogues **9b-d**, the introduction of an amide linker into C3 position (**21a** and **21b**) resulted in loss of kinase inhibition (all IC_{50} > 1 µM). The same modification in the position C5 was better tolerated, however analogues **17a** and **17b** inhibited DYRK1A with higher IC_{50} values (344 and 127 nM, respectively). The finding that C3-modified analogues failed to inhibit all kinases underlines the importance of the C3 phenolic group attached to the 7-azaindole core. The C5 position, however, offered scope for improvement of activity and yielded analogues **9h** and **10a** with low nanomolar potency.

CELL-BASED SCREENING

Glioblastoma is a heterogeneous cancer with great variability between patients and even within the same patient. Glioblastoma tumors have been sub-classified into four molecular subtypes - classical, proneural, neural and mesenchymal.[52] Each subtype is characterized by distinct molecular traits; however, the established glioblastoma cell lines inadequately mirror genotypes and phenotypes seen in glioblastoma patients. Accordingly, we observed that the established U251 and A172 glioblastoma cell lines express higher quantities of DYRK1A than the patient-derived glioblastoma cell lines RN1, JK2, WK1 and SJH1 (Figure 1A). As DYRK1A activity correlates with the protein quantity, higher DYRK1A quantity (thus higher DYRK1A activity) in the established glioblastoma cells could render these cells more sensitive to DYRK1A inhibition, however, would not be clinically relevant. Furthermore, DYRK1B, DYRK2, CLK1 expression pattern in patient-derived glioblastoma cells also differs from the profile of U251 and A172 cells (Figure 1A). With the exception of SJH1 cells that express only DYRK1A; the RN1, WK1 and JK2 cells express also DYRK1B, DYRK2 and CLK1 - albeit to a lesser degree than DYRK1A expression. We have therefore chosen to screen all inhibitors in patient-derived glioblastoma cells. These cells were grown as stem cells under defined conditions in order to maintain the phenotype and genotype of the primary resected tumors (Figure 1B).[53,54, 55] Viability of cells treated with test compounds was determined in the Alamar blue assay (Table 1 - 3).

A

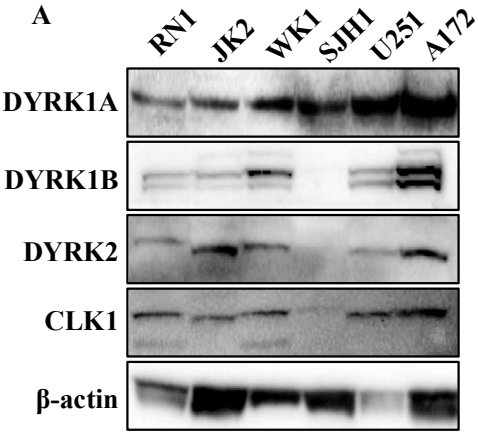

B

Cell line	Subtype	Genotype
RN1	Classical	p53wt, CDKN2A null, PTENwt
JK2	Proneural	p53 mut, CDKN2A null, PTENwt
WK1	Mesenchymal	p53 wt, CDKN2A null, PTEN null
SJH1	Neural	p53 mut, CDKN2A null, PTENwt, NF1 mut

Figure 1. Expression of DYRK/CLK1 kinases and genotype of patient-derived glioblastoma cell lines. (A) Cell lysate of untreated cells were analyzed with Western blotting using indicated antibodies (representative image of 2 independent blots). **(B)** Subtype and genotype of patient-derived glioblastoma cell line RN1, JK2, WK1 and SJH1 as previously described[54, 55].

The lead compound **3a** reduced viability of RN1 cells with EC_{50} of 2.0 μM (Table 1). The two most potent kinase inhibitors developed in this study, compounds **9h** and **10a** reduced RN1 viability with 1.1 μM and 2.1 μM potency, respectively (Table 2). Compounds **10b** and **10c**, inhibiting DYRK1A, DYRK1B, DYRK2 and CLK1 with potencies (9.6 – 724 nM) comparable to **9h** were 13-fold less efficacious in the cell viability assays (EC_{50} > 13 μM) compared to **9h** (EC_{50} = 1.1 μM). This reduction in efficacy could arise from the increased polarity and reduced cell membrane permeability, however, off-target effects could also be playing a role. For the remaining compounds, cellular efficacy correlated with the potency in the kinase inhibition assay.

For example, compounds **10b** and **17b** with nanomolar kinase inhibition activity (IC_{50} = 26 - 644 nM) reduced RN1 viability with mid-range micromolar potency (EC_{50} > 10 μM), whereas compounds lacking kinase inhibition activity, e.g. **3b**, **9d**, **21b** (IC_{50} > 1 μM) were not cytotoxic to RN1 cancer cells up to 50 μM (Table 1 and Table 3).

This trend in SAR was also observed in WK1, JK2 and SJH1 cells, and DYRK1A inhibition activity correlated with the cellular efficacies (R = 0.71, 0.63, 0.60 and 0.69 for DYRK1A (IC_{50}) *vs* RN1, WK1, JK and SJH1 (EC_{50}), respectively; Spearman correlation). The most efficacious compounds across all cell lines were compounds **9h** and **10a**, with the classical RN1 and mesenchymal WK1 cells being most responsive to these inhibitors (EC_{50} = 0.9 – 2.1 μM). Viability of the neural SJH1 and proneural JK2 cell lines was reduced by **9h** and **10a** with the EC_{50} values ranging 3.2 - 8.6 μM.

CELL-BASED FUNCTIONAL EVALUATION

To evaluate the most potent inhibitors further, we tested analogues **9h** and **10a** in several cell-based assays. As a negative control, we employed analogue **9d** that lacks the kinase inhibition activity and

was not cytotoxic to primary cells (Table 1). Accordingly, analogue **9d** did not reduce viability of established A172 and U251 glioblastoma cell lines (EC_{50} > 50 μM), whereas **9h** and **10a** decreased A172 and U251 viability with efficacies ranging 1.6 – 4.6 μM.

Cellular thermal shift assay (CETSA). To demonstrate target engagement in cells, compound **9h** was assessed for its ability to penetrate cells and bind to DYRK1A in a manner that was independent of a phenotypic end point (*i.e.* reduced cell viability). For this, we used a cellular thermal shift assay (CETSA)[56, 57] to assess DYRK1A engagement in U251 cells as this cell line expresses high quantities of DYRK1A. In brief, U251 cells were treated with analogue **9h** (10 μM) and cell suspensions were heated to different temperatures to induce protein denaturation. Soluble proteins were extracted with an aqueous buffer and analyzed with Western blotting. Inhibitors that bind to their cognate target in cells would yield a stabilized protein, which will be detected at higher temperatures compared to the denaturation profile in cells without drug treatment. Indeed, **9h** efficiently stabilized DYRK1A, but not p38α MAPK (Figure 2A-B), validating that this inhibitor binds to cellular DYRK1A and most likely the related DYRK1B, DYRK2 and CLK1 kinases; whereas the stability of the structurally unrelated p38α MAPK was not affected by **9h**. To investigate **9h** concentration effects, we derived the isothermal dose-response fingerprint ($ITDRF_{CETSA}$), which is a characteristic ligand-induced protein stabilization at a constant temperature. In this experiment, the DYRK1A biochemical potency of **9h** (IC_{50} = 43 nM) translated well into its cellular target engagement ($ITDFR_{CETSA}$ = 711 nM; Figure 2C-D).

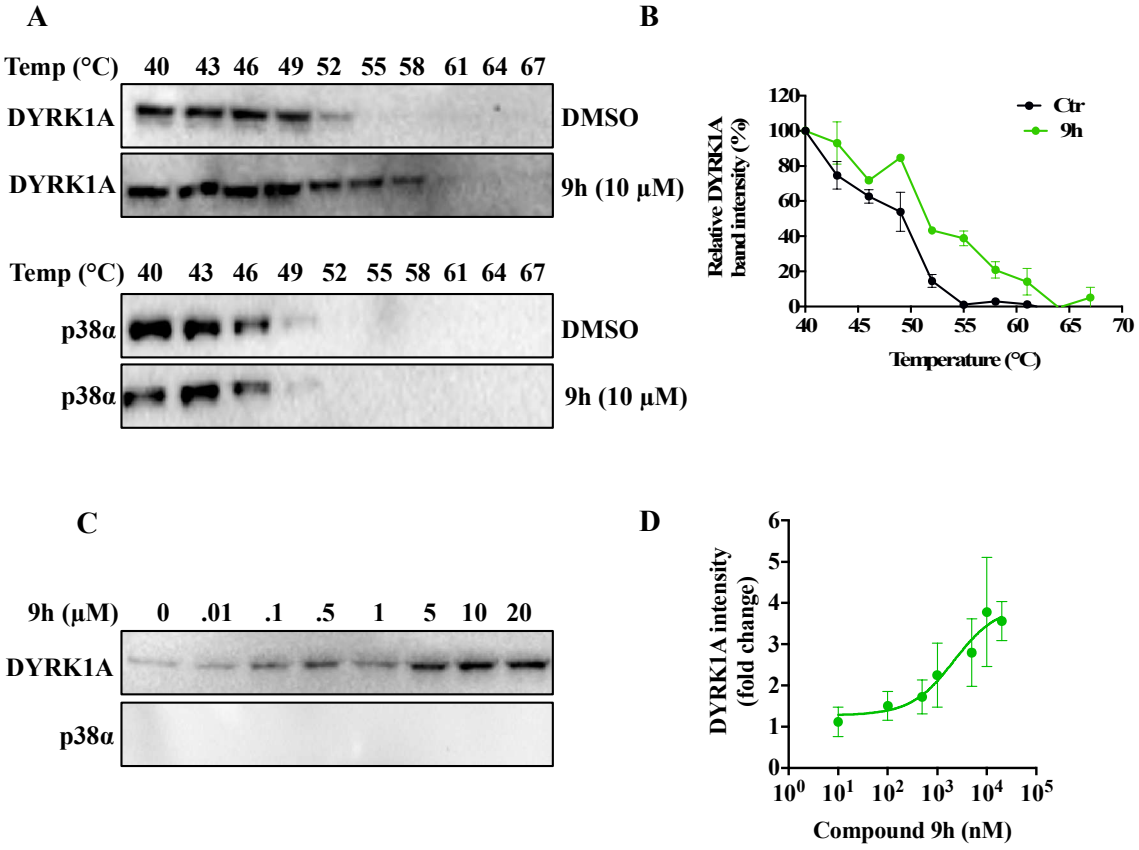

Figure 2. Treatment of U251 cells with inhibitor 9h stabilizes DYRK1A and decreases cell viability. CETSA melt curves (40 – 67 °C) for DYRK1A and p38α (**A**) and quantification (mean ± SEM) of 3 independent experiments (**B**) were determined in intact U251 cells treated with compound **9h** (1 h, 10 µM). Representative image (**C**) and quantification (mean ± SEM) of 2 independent experiments (**D**) of $ITDRF_{CETSA}$ in intact U251 cell treated with compound **9h** (0 - 20 µM, 1 h) at 54 °C.

EGFR degradation. To further confirm DYRK1A inhibition in cells treated with **9h**, we performed a EGFR degradation assay. EGF binding to EGFR induces dimerization and mutual phosphorylation. The phosphorylated EGFR dimer activates signaling pathways to stimulate cell proliferation. EGFR dimerization also triggers endocytosis and lysosomal degradation of EGFR. DYRK1A over-expression has been shown to block this pathway of EGFR degradation, resulting in

longer half-life of EGFR protein.[27] Thus, in cells where DYRK1A is inhibited, EGFR is expected to degrade at a faster rate compared to untreated cells. We therefore tested **9h** for its ability to increase EGFR degradation in U251 cells. EGFR protein translation was blocked with cyclohexamide and EGFR degradation was induced with EGF (100 ng/mL). Cell lysates were collected at indicated time points and the amount of non-degraded EGFR quantified by Western blotting (Figure 3A). Basal EGFR half-life ($t_{1/2}$) in untreated U251 cells was 25.6 ± 7.6 min. Pre-treatment of cells with **9h** (2.5 μM) reduced EGFR half-life to 11.3 ± 2.5 min (Figure 3B). Importantly, a similar effect was observed with genetic knock-down of DYRK1A. Using *si*RNA approach, we achieved on average 80% reduction in DYRK1A expression (Figure 3C) and this DYRK1A down-regulation reduced EGFR half-life to 3.3 ± 2.5 min (Figure 3D).

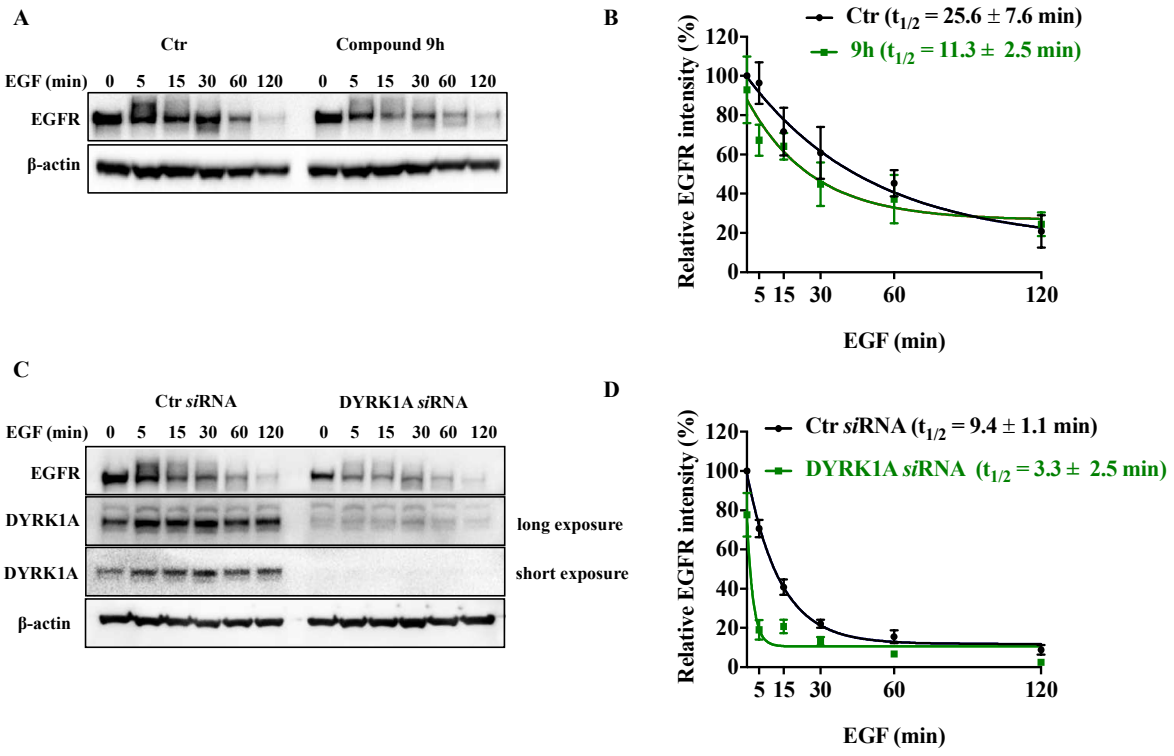

Figure 3. DYRK1A inhibition induces EGFR degradation. (**A**) U251 cells were treated with DMSO (Ctr) or compound **9h** (2.5 μM) for 4 h. Cells were incubated with cycloheximide (30 μg/mL; 1 h) and EGF (100 ng/mL) was added for indicated time points. (**B**) U251 cells were treated with scramble (Ctr) or DYRK1A-targeting *si*RNa for 24 h. Cells were incubated with cycloheximide (30 μg/mL; 1 h) and EGF (100 ng/mL) was added for indicated time points. Cell lysates were analyzed

by Western Blotting using indicated antibodies. (**C** - **D**) EGFR levels were normalized to loading control (β-actin) and are expressed as percentage of untreated cells (0 min). Half-life ($t_{1/2}$) values were calculated by non-linear regression analysis and represent mean ± SEM from 3 independent experiments.

Clonogenic survival. Based on kinase inhibition *in vitro* and in cells, we evaluated compounds **9h** and **10a** for their ability to reduce long-term survival of glioblastoma cells. Compounds **9h** and **10a** dose-dependently inhibited clonogenic survival of RN1 with EC_{50} values of 0.8 and 2.1 μM (Figure 4A-B), respectively; mirroring the EC_{50} values obtained in the short-term viability assay (Table 2). Compound **9h** was more efficacious at reducing the survival of the established U251 cell line (EC_{50} = 0.18 μM, Figure 4C).

As numerous kinase inhibitors, including inhibitors targeting DYRK1B[58], directly bind tubulin and act as tubulin inhibitors, we tested compounds **9h** and **10a** together with the inactive analogue **9d** for their potential effect on tubulin polymerization *in vitro*. None of the tested compounds altered the rate of tubulin polymerization, whereas the tubulin-targeting agents paclitaxel and vinblastine changed the rate of tubulin polymerization in agreement with their established mechanism of action (data not shown).

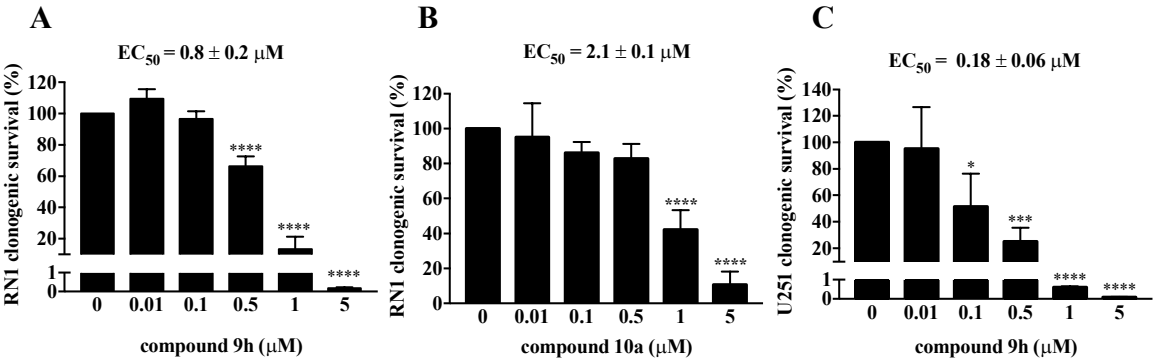

Figure 4. Clonogenic survival following drug treatment. Patient-derived RN1 glioblastoma cells were treated with **9h** (**A**) or **10a** (**B**) for 10 days. Established U251 glioblastoma cells were treated with **9h** (**C**) for 10 days. Colonies were fixed, stained with Toluidine Blue and counted using the ImageJ software. Data were normalized to vehicle-treated controls (set as 100% survival) and EC_{50}

values calculated by non-linear regression analysis. EC_{50} values represent mean ± SEM from 3 independent experiments performed in duplicate. One-way ANOVA, followed by Dunnett's multiple comparison test was used to determine statistical significance. (*P < 0.05, *** P < 0.001, ****P < 0.0001 in relation to vehicle-treated cells).

Migration and invasion. We assessed **9h** and **10a**, together with the inactive structural analogue **9d** using *in vitro* assays of cell migration and invasion (Table 4). In the migration assay, the movement across the wound is measured, whereas in the invasion assay the motility through the wound coated with Matrigel is measured. We employed U251, A172 and RN1 cell lines, all of which show high basal velocity (υ) of migration (υ > 2,000 μm/h) and invasion (υ > 1,000 μm/h). The inhibitor **9h** potently reduced migration of A172, U251 and RN1 cells, with more than 75% inhibition of migration reached at 5 μM concentration (Table 4). This inhibitor also blocked invasiveness of A172 and U251 cells in a dose-dependent manner (Table 4). Similar effects were observed across all assays with the analogue **10a**, whereas the inactive analogue **9d** that lacks DYRK/CLK kinase inhibition activity (Table 1) was ineffective in the migration and invasion assays (Table 4).

Table 4. Inhibition of migration and invasion of glioblastoma cells by CMGC inhibitors **9h** and **10a**, and inactive analogue **9d**. Values represent mean ± SEM from 3 independent experiments.

	Conc. (μM)	U251 migration ($\dot{v}$, μm/h)	U251 invasion ($\dot{v}$, μm/h)	A172 migration ($\dot{v}$, μm/h)	A172 invasion ($\dot{v}$, μm/h)	RN1 migration ($\dot{v}$, μm/h)
9h	0.0	2,163 ± 133	1,337 ± 93	3,123 ± 103	2,659 ± 674	1,174 ± 158
	1.0	1,247 ± 176	1,139 ± 112	2,828 ± 271	2,675 ± 475	355 ± 28
	5.0	127 ± 56	234 ± 22	728 ± 308	1,538 ± 696	118 ± 43
	10.0	129 ± 52	-149 ± 12	131 ± 129	714 ± 585	208 ±77
10a	0.0	2,159 ± 48	1,710 ± 97	2,739 ± 428	3,047 ± 506	1,115 ± 110
	1.0	1,125 ± 93	736 ± 117	2,891 ± 147	2,731 ± 431	332 ± 33
	5.0	173 ± 38	34 ± 153	2,296 ± 564	2,027 ± 419	210 ± 64
	10.0	111 ± 1	-118 ± 37	651 ± 300	1,718 ± 517	196 ± 47
9d	0.0	2,653 ± 395	1,151 ± 133	2,650 ± 675	2,990 ± 997	937 ± 17
	1.0	2,331 ± 143	1,451 ± 69	3,123 ± 745	2,411 ± 241	1,070 ± 246
	5.0	2,370 ± 39	1,481 ± 181	3,065 ± 718	2,232 ± 498	929 ± 253
	10.0	2,702 ± 239	1,380 ± 73	2,827 ± 709	2,707 ± 491	791 ± 236

CONCLUSION

DYRK1B and DYRK2 have been recently implicated in the progression of various cancers,[33, 37] however the therapeutic potential of simultaneously targeting DYRK kinases has not been evaluated. The hypothesis that inhibition of DYRK protein family would have anti-cancer efficacy was tested in this study, with glioblastoma being an example of a tumor type where a strong response might be expected. Glioblastoma cells up-regulate DYRK1A, and the link between DYRK1A over-expression and glioblastoma pathogenesis has been established *in vivo*.[3, 27] To address the therapeutic potential of simultaneously targeting DYRK kinases, all of which are variously expressed in glioblastoma subtypes, a series of potent and cell-active DYRK inhibitors have been developed and profiled in biochemical and glioblastoma cell-based models.

While others have concentrated on the development of selective DYRK1A inhibitors,[17, 18] our goal was to understand SAR across the DYRK family. Using compounds within and across series that exhibit a full spectrum of potencies, we demonstrate that the SAR established for inhibition of DYRK1A is nearly identical to that for DYRK1B inhibition. This observation is not surprising as these two DYRK isoforms share high degree of homology, with only one amino acid difference in the ATP binding pocket.[59] However, while the 7-azaindole-based scaffold explored in this study offers little opportunity for developing selective DYRK1A inhibitors, quinolone-6-carboxylic acid derivatives have been developed into highly selective DYRK1A inhibitors,[17] demonstrating that within the CMGC family of protein kinases selective inhibition of DYRK1A is possible. Numerous DYRK1A inhibitors potently bind to and inhibit the related CLK family kinases[13, 60] and this has been also demonstrated in our study. The potency of tested analogues to inhibit DYRK1A and DYRK1B activity was comparable to the potency of inhibitors against CLK1; with exception of compound **10c** which inhibited CLK1 with >2-fold higher potency than DYRK1A/B. Nevertheless, CLK1 inhibition offers a therapeutic advantage as alternative splicing driven by excessive CLK1 activity drives numerous hallmarks of cancer.[32] Finally, all inhibitors inhibited DYRK2 with >10-fold higher IC_{50} values.

To address the clinical potential of these novel DYRK inhibitors, their cellular efficacy was assessed in patient-derived glioblastoma cells. Our screening platform considers both the diversity between patients and the heterogeneity of cells within a patient, and allowed us to identify not only the most efficacious inhibitors from the series, but also the glioblastoma subtype most sensitive to the inhibition of DYRK and CLK family of kinases. We established a correlation between biochemical and cellular activities across the series, and confirmed that the anti-proliferative activity is not a result of a tubulin targeting effect. However, the role of other kinases and non-kinase targets cannot be completely discounted, as the proteome profile of the lead inhibitors is unknown at this stage of the project (?). Nevertheless, the most potent DYRK/CLK inhibitors attenuated viability of glioblastoma cells with low micromolar potency; and RN1 and WK1 cells

were most sensitive to inhibitors **9h** and **10a**,. These two cell lines represent the classical (60%) and mesenchymal (13%) glioblastoma tumors, respectively; thus, our data suggests that DYRK/CLK-targeted therapy could be beneficial for majority of patients diagnosed with glioblastoma.

To further demonstrate the anti-cancer potential, inhibitor **9h** was evaluated in the EGFR degradation, clonogenic cell survival, migration and invasion assays. In all assays, compound **9h** was efficacious in the low micromolar range. Although the cellular efficacy and biochemical IC_{50} values differ, several factors must be taken into consideration when translating the potency values obtained in kinase inhibition assays to the activity of inhibitors in cells. Firstly, kinase inhibition assays are performed with recombinant, pre-activated enzymes and a large excess of the phosphoacceptor, which renders kinases more sensitive to the inhibitor.[61] Secondly, for the ATP competitive kinase inhibitors (such as those developed in this study), the IC_{50} value depends on the competition from ATP under the assay conditions. We performed all kinase assays at 100 μM ATP, based on the K_M(ATP) value for DYRK1A (30 μM). However, when the ATP concentration exceeds the K_M(ATP), the IC_{50} value increases as well. As the ATP concentration in cells is in the 1-5 mM range, an inhibitor concentration that is higher than the IC_{50} value determined from biochemical kinase inhibition assays will be required to inhibit the targeted kinase in the cell. It is suggested that an ATP-competitive kinase inhibitor should be active in cells at a concentration approximately 10 to 100-fold above its IC_{50} value as determined in biochemical assays using the K_M(ATP) concentration.[62] In the cellular assays, efficacy of **9h** was significant in the 0.8 – 2.5 μM range, which is 20 to 70-fold above the biochemical IC_{50} values for the inhibition of DYRK1A, DYRK1B and CLK1 (34 – 43 nM).

In addition to using an appropriate inhibitor concentration in the functional studies and CETSA assays, we demonstrate that genetic knock-down of DYRK1A induced EGFR degradation comparable to the degradation kinetics determined upon pharmacological DYRK1A inhibition with compound **9h**. Together, these data imply DYRK1A as a kinase responsible for EGFR stabilization. However, as DYRK1A knock-down had only mild effects on cell viability (data not shown) we

conclude that the anti-proliferative efficacy of inhibitor **9h** is due to simultaneously targeting the DYRK-CLK family of kinases, though other off-target effects could also be a factor. In summary, the protein kinases of the DYRK family are emerging as potential targets for small molecule cancer therapy. We present a library of novel potent and cell-active DYRK kinase inhibitors to further explore the role of the DYRK kinases in an *in vivo* glioblastoma model setting.

EXPERIMENTAL SECTION

General chemical synthesis details

Unless noted otherwise, commercially obtained reagents were used as purchased without further purification. Solvents for flash chromatography were distilled prior to use, or used as purchased for HPLC grade, with the eluent mixture reported as the volume/volume ratio (v/v). Flash chromatography was performed using Merck Kieselgel 60 (230–400 mesh) silica gel. Analytical thin-layer chromatography was performed using Merck aluminum-backed silica gel 60 F254 (0.2 mm) plates (Merck, Darmstadt, Germany), which were visualized using shortwave (254 nm) ultraviolet fluorescence. Melting points were measured with a rate of 6 °C/min and are uncorrected. Infrared absorption spectra were reported as vibrational frequency (cm^{-1}). Nuclear magnetic resonance spectra were recorded at 300 K using a 200 MHz, 300 MHz, 400 MHz or a 500 MHz spectrometer. The data are reported as chemical shift (δ ppm) relative to the residual protonated solvent resonance, relative integral, multiplicity (s = singlet, br.s = broad singlet, d = doublet, dd = doublet of doublets, t = triplet, m = multiplet, etc.) and coupling constants (*J* Hz). Low resolution mass spectra (LRMS) was obtained from a ThermoQuest Finnigan LCQ Deca ion trap mass spectrometer with electro-spray ionization in either positive (+ESI) or negative (-ESI) mode. Data is expressed as observed mass (m/z), assignment (M = molecular ion), and relative intensity (%). High resolution mass spectra was performed on a Bruker Apex Qe 7T Fourier Transform Ion Cyclotron Resonance mass spectrometer equipped with an Apollo Π ESI dual source. Samples were run with syringe infusion at 150 μL/hr on a Cole Palmer syringe pump into electrospray ionization (ESI). High performance liquid chromatography (HPLC) analysis of organic purity was conducted on a Waters Alliance 2695 instrument using a SunFire™ C18 column (5 μm, 2.1 x 150 mm) and detected using a Waters 2996 photodiode array (PDA) detector set at 254 nm. Separation was achieved using water (solvent A) and acetonitrile (solvent B) at flow rate of 0.2 mL/min and a gradient of 0% B to 100% or 40% over 30 min. HPLC data is reported as percentage purity (≥95%) and retention time (RT) in minutes.

General procedure A: synthesis of 5-bromo-3-iodo-1-tosyl-based derivatives

The compounds ware prepared according to the literature.[13] To a solution of indole-based compound **4a-c** (1.00 equiv) in CH_2Cl_2 (0.05 M) was added KOH (0.50 equiv) at RT. After 30 min, *N*-iodosuccinimide (1.00 equiv) was added, the mixture was stirred for 10 h, quenched with a saturated solution of $Na_2S_2O_3$ and extracted with CH_2Cl_2. The combined organic layers were dried ($MgSO_4$) and concentrated in *vacuo*. The desired product was used in the next step without further purification.

To a solution of **5a-c** (1.00 equiv) in CH_2Cl_2 (0.05 M) were added sodium hydride 60% (3.00 equiv) and benzyltriethylammonium chloride (0.02 equiv) under argon at 0 °C. After 30 min, 4-methylbenzenesulfonyl chloride (1.20 equiv) was added at 0 °C, and the mixture was stirred at RT. After 2 h, water was added and extracted with CH_2Cl_2. The combined organic layers were dried ($MgSO_4$) and concentrated in *vacuo*.

General procedure B for di-Suzuki Coupling Reaction: To a solution of **6a-c** (1.00 equiv) in toluene/ethanol 3:1 (0.02 M) were added (4-methoxyphenyl)boronic acid (2.00 equiv), K_2CO_3 (2 M solution in water, 4.00 equiv), and $Pd(PPh_3)_4$ (4 mol %), and the reaction was heated to 110 °C for 5 h under argon. The reaction mixture was cooled to room temperature, concentrated in *vacuo*, and then partitioned between water and ethyl acetate. The aqueous layer was extracted with ethyl acetate, and the combined organic layers were dried ($MgSO_4$) and concentrated in *vacuo*. The residue was purified using flash chromatography (hexane/ethyl acetate 5:1 → 3:1) to give the product.

General procedure C for mono-Suzuki Coupling Reaction: To solution of **6a** or **7d-g** or **16a-b** or **19a-b** (1.00 equiv) in toluene/ethanol 3:1 (0.02 M) were added arylboronic acid (1.00 equiv), K_2CO_3 (2 M solution in water, 2.00 equiv), and $Pd(PPh_3)_4$ (2 mol %), and the reaction was heated to 90 °C for 3 h under argon. The reaction mixture was cooled to room temperature, solvent was

removed under reduce pressure, and then partitioned between water and ethyl acetate. The aqueous layer was extracted with ethyl acetate, and the combined organic layers were dried ($MgSO_4$) and concentrated *in vacuo.*

General procedure D for the synthesis of tetrazole: To a solution of cyanated compound **8f** or **8i** (1.00 equiv) in *t*-BuOH and H_2O (1:1 v/v, 0.125 M), were added TBAF (1 M in THF, 1.00 equiv), trimethylsilyl azide (10.00 equiv), $CuSO_4 \bullet 5H_2O$ (0.01 equiv) and sodium ascorbate (0.03 equiv), and the mixture was stirred at 80 °C under microwave irradiation (100 W) for 2 h. The mixture was quenched with water and extracted with ethyl acetate (3 x 10 ml), the combined organic layers were dried ($MgSO_4$) and concentrated under reduced pressure.

General procedure E for deprotection of tosyl-group: To a solution of **7a-c**, **8d-k** or **14a-b** (1.00 equiv) in MeOH (0.02 M) was added KOH (5.00 equiv), and the reaction was heated to 80 °C for 2 h. After completion, the solvent was removed under reduced pressure, and then partitioned between water and ethyl acetate. The aqueous layer was extracted with ethyl acetate, and the combined organic layers were dried ($MgSO_4$) and concentrated *in vacuo*.

General procedure F for demethylation: To a solution of **8a-c** (1.00 equiv) in dry CH_2Cl_2 (0.05 M) was added BBr_3 (1M solution in CH_2Cl_2, 6.00 equiv) under nitrogen. The reaction mixture was stirred at room temperature for 15 h, then quenched at 0 °C with MeOH and concentrated *in vacuo*.

General procedure G for reduction of nitro compounds. To a solution of **9a** or **9e** (1.00 equiv) in HCl (3N solution in water, 0.03 M) was added iron powder (10.00 equiv), and the reaction was heated to 110 °C for 3 h. After completion and cooling down, the mixture was neutralized with $NaHCO_3$ (aq), and extracted with ethyl acetate, and the combined organic layers were dried ($MgSO_4$) and concentrated *in vacuo*.

General procedure H for the protection of 4- or 3-hydroxyaniline with *tert*-Butyldimethyl group[63]: To a solution of 4-hydroxyaniline or 3-hydroxyaniline (1.00 equiv, 5 mmol) in dry DMF (0.05 M) was added imidazole (2.50 equiv, 12.5 mmol) at 0 °C, followed by the addition of TBSCl (1.50 equiv, 7.5 mmol). The reaction mixture was stirred at RT for 12 h, after completion monitored by TLC, the mixture was extracted with ethyl acetate (3 x 30 mL) and water (50 mL), the organic layers were dried ($MgSO_4$) and concentrated *in vacuo*.

General procedure I for amide coupling reaction of aromatic acid and substituted aniline: To a solution of acid **12** or **18** (1.00 equiv) in DMSO (0.05 M) was added HBTU (1.20 equiv) under nitrogen at 0 °C, followed by the addition of DIPEA (2.50 equiv) and aniline **13a** or aniline **13b** (1.10 equiv). The reaction mixture was stirred at RT for 2 h. after completion monitored by TLC, the mixture was extracted with ethyl acetate and H_2O, the organic layers were dried ($MgSO_4$) and concentrated *in vacuo*. The residue was purified by flash chromatography (hexane/ethyl acetate 5:1 → 3:1) to give the product.

4,4'-(1*H*-pyrrolo[2,3-*b*]pyridine-3,5-diyl)diphenol (3a). This compound was prepared according to **General procedure F.** The residue was purified by flash chromatography (CH_2Cl_2/MeOH 100:1 → 50:1) to give the product as a pale yellow solid (65% yield). R_f (CH_2Cl_2/MeOH 20:1): 0.45; **^{1}H NMR** (500 MHz, DMSO-*d*): δ 11.83 (1H, s), 9.69-9.23 (1H, br s), 8.47 (1H, d, J = 2.0 Hz), 8.30 (1H, d, J = 2.0 Hz), 7.71 (1H, d, J = 2.5 Hz), 7.56 (4H, dd, J = 0.9 Hz, J = 8.6 Hz), 6.87 (4H, dq, J = 2.0 Hz, J = 8.6 Hz), one OH signal not observed; **^{13}C NMR** (125 MHz, DMSO-*d*): δ 156.8, 155.7, 147.2, 140.5, 129.5, 128.7, 128.2, 127.7, 125.6, 125.3, 123.2, 117.9, 115.8, 115.7, 115.0; **HRMS** (ESI+) calcd for $C_{19}H_{14}N_2O_2$ $[M + H]^+$ 303.1128, found 303.1130. **IR** (neat, cm^{-1}): $\tilde{\nu}$ 3107, 2943, 1611, 1249. **HPLC**: 98.9%, RT: 16.4 mins.

4,4'-(1*H*-indole-3,5-diyl)diphenol (3b). This compound was prepared according to **General procedure F.** The residue was purified by flash chromatography (CH_2Cl_2/MeOH 100:1 → 50:1) to give the product as a white solid (60% yield). m.p. 246-248 °C; R_f (CH_2Cl_2/MeOH 20:1): 0.50; **^{1}H NMR** (500 MHz, MeOD): δ 7.90 (1H, d, J = 1.0 Hz), 7.48 (4H, dd, J = 8.6 Hz, J = 23.2 Hz), 7.42 (1H, d, J = 8.5 Hz), 7.35-7.33 (2H, m), 6.86 (4H, dd, J = 8.5 Hz, J = 14.8 Hz), NH and OH signals not observed; **^{13}C NMR** (125 MHz, MeOD): δ 157.2, 156.5, 137.6, 135.8, 134.2, 129.4, 129.1, 129.0, 127.6, 123.1, 122.0, 118.6, 117.9, 116.5, 116.4, 112.6; **HRMS** (ESI+) calcd for $C_{20}H_{15}NO_2$ $[M + Na]^+$ 324.0995, found 324.0998. **IR** (neat, cm^{-1}): $\tilde{\nu}$ 3402, 3022, 1514, 1219, 1170, 798. **HPLC**: >99.9%, RT: 21.7 mins.

4,4'-(1*H*-indazole-3,5-diyl)diphenol (3c). This compound was prepared according to **General procedure F.** The residue was purified by flash chromatography (CH_2Cl_2/MeOH 100:1 → 50:1) to give the product as a white solid (58% yield). m.p. 251-252 °C; R_f (CH_2Cl_2/MeOH 20:1): 0.50; **^{1}H NMR** (500 MHz, MeOD): δ 8.11 (1H, s), 7.97 (1H, d, J = 8.7 Hz), 7.82 (2H, d, J = 7.4 Hz), 7.73 (1H, d, J = 8.7 Hz), 7.51 (2H, d, J = 7.4 Hz), 7.06 (2H, d, J = 7.4 Hz), 6.89 (2H, d, J = 7.2 Hz), NH and OH signals not observed; **^{13}C NMR** (125 MHz, MeOD): δ 161.6, 158.7, 144.6, 141.4, 139.2, 133.2, 132.6, 131.1, 129.5, 120.3, 119.6, 119.5, 117.7, 116.9, 112.9; **HRMS** (ESI+) calcd for $C_{19}H_{14}N_2O_2$ $[M + H]^+$ 303.1128, found 303.1131. **IR** (neat, cm^{-1}): $\tilde{\nu}$ 3343, 2980, 1609, 1497, 1263, 1182, 809, 507. **HPLC**: 98.8%, RT: 19.9 mins.

5-bromo-3-iodo-1-tosyl-1*H*-pyrrolo[2,3-*b*]pyridine (6a). This compound was prepared according to **general procedure A**. The residue was purified using flash chromatography (hexane/ethyl acetate 15:1 → 10:1) to give the product as a white solid (81% yield over two steps). m.p. 186-187 °C; R_f (hexane/ethyl acetate 10:1): 0.65; **^{1}H NMR** (500 MHz, $CDCl_3$): δ 8.44 (1H, d, J = 2.1 Hz), 8.06-8.04 (2H, m), 7.86 (1H, s), 7.78 (1H, d, J = 2.1 Hz), 7.29 (2H, d, J = 8.1 Hz), 2.37 (3H, s); **^{13}C NMR** (125 MHz, $CDCl_3$): δ 146.7, 146.0, 144.7, 134.7, 132.5, 131.4, 130.0, 128.4, 126.7, 116.0,

60.4, 21.8; **LRMS** (+ESI): *m/z* 499/501 (100/97, $[M + Na]^+$). IR (neat, cm^{-1}): $\tilde{\nu}$ 3138, 1619, 1371, 1167, 1140, 1015, 527. The spectroscopic data matched that reported in the literature[41].

5-bromo-3-iodo-1-tosyl-1H-indole (6b). This compound was prepared according to **general procedure A**. The residue was purified using flash chromatography (hexane/ethyl acetate 20:1 → 10:1) to give the product as a white solid (89% yield over two steps). **^{1}H NMR** (200 MHz, $CDCl_3$): δ 7.83 (1H, d, J = 8.7 Hz), 7.75 (2H, d, J = 8.4 Hz), 7.68 (1H, s), 7.51 (1H, d, J = 1.7 Hz), 7.45 (1H, dd, J = 1.9 Hz, J = 8.7 Hz), 7.25 (2H, d, J = 8.0 Hz), 2.36 (3H, s); **^{13}C NMR** (50 MHz, $CDCl_3$): δ 145.8, 134.8, 134.4, 133.3, 131.1, 130.3, 128.8, 127.1, 125.0, 117.7, 115.0, 65.5, 21.8. The spectroscopic data matched that reported in the literature[64].

5-bromo-3-iodo-1-tosyl-1*H*-indazole (6c). This compound was prepared according to **general procedure A**. The residue was purified using flash chromatography (hexane/ethyl acetate 20:1 → 10:1) to give the product as an off-white solid (80% yield over two steps). m.p. 160-161 °C; R_f (hexane/ethyl acetate 12:1): 0.50; **^{1}H NMR** (500 MHz, $CDCl_3$): δ 8.05 (1H, dd, J = 0.5 Hz, J = 8.9 Hz), 7.86 (2H, dd, J = 1.7 Hz, J = 6.7 Hz), 7.69 (1H, dd, J = 1.8 Hz, J = 8.9 Hz), 7.60 (1H, d, J = 1.6 Hz), 7.27 (2H, d, J = 8.1 Hz), 2.38 (3H, s); **^{13}C NMR** (125 MHz, $CDCl_3$): δ 146.2, 139.2, 134.1, 133.5, 131.9, 130.2, 127.9, 125.0, 118.2, 114.8, 102.4, 21.8; **LRMS** (+ESI): *m/z* 499/501 (100/86, $[M + Na]^+$). **IR** (neat, cm^{-1}): $\tilde{\nu}$ 3102, 3071, 2923, 1593, 1373, 1238, 663, 531.

3,5-bis(4-methoxyphenyl)-1-tosyl-1*H*-pyrrolo[2,3-*b*]pyridine (7a). This compound was prepared according to **general procedure B** to give the product as a white solid (87% yield). m.p. 158-160 °C; R_f (hexane/ethyl acetate 2:1): 0.45; **^{1}H NMR** (400 MHz, $CDCl_3$): δ 8.64 (1H, d, J = 2.1 Hz), 8.14 (2H, d, J = 2.0 Hz), 8.12 (1H, d, J = 1.8 Hz), 7.81 (1H, s), 7.54 (2H, dd, J = 2.2 Hz, J = 6.7 Hz), 7.49 (2H, dd, J = 2.2 Hz, J = 6.7 Hz), 7.29 (2H, dd, J = 0.6 Hz, J = 8.6 Hz), 7.01 (4H, dt, J = 2.2 Hz, J = 8.8 Hz), 3.87 (3H, s), 3.85 (3H, s), 2.38 (3H, s); **^{13}C NMR** (100 MHz, $CDCl_3$): δ 159.6,

159.5, 146.8, 145.3, 144.2, 135.7, 132.7, 131.1, 129.8, 128.9, 128.7, 128.2, 126.8, 125.3, 122.7, 122.0, 120.4, 114.8, 114.7, 55.5 (two overlapping signals), 21.8; **LRMS** (+ESI): *m/z* 507 (100, $[M + Na]^+$). **IR** (neat, cm^{-1}): $\tilde{\nu}$ 2920, 2836, 1596, 1381, 1173, 1157, 577.

3,5-bis(4-methoxyphenyl)-1-tosyl-1*H*-indole (7b). This compound was prepared according to **general procedure B** to give the product as a white solid (86% yield). m.p. 168-170 °C; R_f (hexane/ethyl acetate 2:1): 0.45; **^{1}H NMR** (500 MHz, $CDCl_3$): δ 8.08 (1H, d, J = 10.4 Hz), 7.86 (1H, s), 7.83 (2H, d, J = 8.0 Hz), 7.64 (1H, s), 7.56-7.54 (3H, m), 7.51 (2H, d, J = 8.2 Hz), 7.23 (2H, d, J = 8.0 Hz), 7.02 (2H, d, J = 8.2 Hz), 6.97 (2H, d, J = 8.2 Hz), 3.86 (3H, s), 3.84 (3H, s), 2.34 (3H, s); **^{13}C NMR** (125 MHz, $CDCl_3$): δ 159.3, 159.1, 145.1, 136.9, 135.3, 134.6, 134.0, 130.2, 130.0, 129.2, 128.5, 127.0, 125.6, 124.3, 124.1, 123.0, 118.5, 114.5, 114.3, 114.1, 55.5, 55.4, 21.7; **LRMS** (+ESI): *m/z* 484 (8, $[M+H]^+$), 506 (100, $[M+Na]^+$). **IR** (neat, cm^{-1}): $\tilde{\nu}$ 2954, 2932, 2834, 1609, 1367, 1170, 835, 576.

3,5-bis(4-methoxyphenyl)-1-tosyl-1*H*-indazole (7c). This compound was prepared according to **general procedure B** to give the product as a white solid (84% yield). m.p. 115-117 °C; R_f (hexane/ethyl acetate 2:1): 0.45; **^{1}H NMR** (400 MHz, $CDCl_3$): δ 8.27 (1H, dd, J = 0.6 Hz, J = 8.8 Hz), 7.98 (1H, dd, J = 0.7 Hz, J = 1.6 Hz), 7.92 (2H, dd, J = 1.7 Hz, J = 6.7 Hz), 7.89 (2H, dd, J = 2.1 Hz, J = 6.8 Hz), 7.75 (1H, dd, J = 1.7 Hz, J = 8.8 Hz), 7.53 (2H, dd, J = 2.1 Hz, J = 6.7 Hz), 7.23 (2H, d, J = 8.0 Hz), 7.01 (4H, ddd, J = 2.1 Hz, J = 6.8 Hz, J = 12.4 Hz), 3.87 (3H, s), 3.85 (3H, s), 2.34 (3H, s); **^{13}C NMR** (100 MHz, $CDCl_3$): δ 160.9, 159.5, 151.9, 145.3, 141.1, 137.9, 134.8, 133.2, 129.9, 129.7, 128.7, 128.6, 127.7, 125.3, 124.1, 119.3, 114.5, 114.4, 113.9, 55.5 (two overlapping signals),, 21.7; **LRMS** (+ESI): *m/z* 507 (100, $[M+Na]^+$), 523 (8, $[M+K]^+$). **IR** (neat, cm^{-1}): $\tilde{\nu}$ 2934, 2836, 1609, 1303, 1274, 837, 589, 578.

5-bromo-3-(4-nitrophenyl)-1-tosyl-1*H*-pyrrolo[2,3-*b*]pyridine (7d). This compound was prepared according to **general procedure C**. The residue was purified by flash chromatography (hexane/ethyl acetate 8:1 → 5:1) to give the product as pale yellow solid (78% yield). m.p. 253-254 °C; R_f (hexane/ethyl acetate 4:1): 0.55; **^{1}H NMR** (500 MHz, $CDCl_3$): δ 8.53 (1H, d, J = 2.1 Hz), 8.34 (2H, dd, J = 2.1 Hz, J = 6.9 Hz), 8.21 (1H, d, J = 2.1 Hz), 8.12 (2H, dd, J = 1.7 Hz, J = 6.7 Hz), 8.03 (1H, s), 7.73 (2H, dd, J = 2.1 Hz, J = 6.9 Hz), 7.32 (2H, d, J = 8.2 Hz), 2.40 (3H, s); **^{13}C NMR** (125 MHz, $CDCl_3$): δ 147.3, 146.5, 146.2, 145.8, 139.0, 134.8, 131.0, 130.1, 128.6, 127.9, 125.7, 124.7, 122.4, 117.4, 116.1, 21.9; **LRMS** (+ESI): *m/z* 494/496 (81/100, $[M+Na]^+$). **IR** (neat, cm^{-1}): $\tilde{\nu}$ 3142, 1597, 1512, 1171, 692.

5-bromo-3-(1*H*-indol-5-yl)-1-tosyl-1*H*-pyrrolo[2,3-*b*]pyridine (7e). This compound was prepared according to **general procedure C**. The residue was purified by flash chromatography (hexane/ethyl acetate 8:1 → 5:1) to give the product as colorless semi-solid (80% yield). R_f (hexane/ethyl acetate 5:1): 0.40; **^{1}H NMR** (500 MHz, MeOD): δ 8.40 (1H, d, J = 2.1 Hz), 8.31 (1H, d, J = 2.1 Hz), 8.03 (2H, d, J = 8.5 Hz), 7.93 (1H, s), 7.77 (1H, d, J = 1.1 Hz), 7.49 (1H, d, J = 8.4 Hz), 7.36 (2H, d, J = 8.2 Hz), 7.33 (1H, dd, J = 1.7 Hz, J = 8.4 Hz), 7.29 (1H, d, J = 3.1 Hz), 6.52 (1H, dd, J = 0.8 Hz, J = 3.1 Hz), 2.36 (3H, s), NH signal not observed; **^{13}C NMR** (125 MHz, MeOD): δ 147.3, 147.2, 146.1, 137.5, 136.4, 132.6, 130.9, 130.0, 129.0, 126.7, 125.2, 124.6, 123.7, 123.2, 122.2, 120.4, 116.4, 112.9, 102.8, 21.6; **LRMS** (+ESI): *m/z* 464/466 (100/98, $[M+H]^+$). **IR** (neat, cm^{-1}): $\tilde{\nu}$ 3401, 2922, 1595, 1382, 1173, 582.

4-(5-bromo-1-tosyl-1*H*-pyrrolo[2,3-*b*]pyridin-3-yl)benzonitrile (7f). This compound was prepared according to **general procedure C**. The residue was purified by flash chromatography (hexane/ethyl acetate 8:1 → 5:1) to give the product as an off-white solid (85% yield). m.p. 219-220 °C; R_f (hexane/ethyl acetate 5:1): 0.45; **^{1}H NMR** (500 MHz, $CDCl_3$): δ 8.52 (1H, d, J = 2.1 Hz), 8.19 (1H, d, J = 2.1 Hz), 8.11 (2H, dd, J = 1.7 Hz, J = 6.7 Hz), 7.98 (1H, s), 7.76 (2H, dd, J =

1.9 Hz, *J* = 6.6 Hz), 7.67 (2H, dd, *J* = 1.9 Hz, *J* = 6.6 Hz), 7.32 (2H, d, *J* = 8.2 Hz), 2.40 (3H, s); **^{13}C NMR** (125 MHz, $CDCl_3$): δ 146.4, 146.1, 145.8, 137.1, 134.8, 133.2, 130.9, 130.0, 128.5, 127.9, 125.4, 122.4, 118.7, 117.8, 116.0, 111.6, 21.9; **LRMS** (+ESI): *m/z* 474/476 (100/68, $[M + Na]^+$), 490 (11, $[M + K]^+$). **IR** (neat, cm^{-1}): $\tilde{\nu}$ 2219, 1607, 1178, 591.

4-(5-bromo-1-tosyl-1*H*-pyrrolo[2,3-*b*]pyridin-3-yl)phenol (7g). This compound was prepared according to **general procedure C**. The residue was purified using flash chromatography (hexane/ethyl acetate 6:1 → 4:1) to give the product as a white solid (80% yield). m.p. 158-168 °C; R_f (hexane/ethyl acetate 4:1): 0.40; **^{1}H NMR** (500 MHz, $CDCl_3$): δ 8.47 (1H, d, *J* = 2.1 Hz), 8.15 (1H, d, *J* = 2.1 Hz), 8.07 (2H, d, *J* = 8.4 Hz), 7.79 (1H, s), 7.42 (2H, dd, *J* = 2.1 Hz, *J* = 6.6 Hz), 7.29 (2H, d, *J* = 8.2 Hz), 6.95 (2H, dd, *J* = 2.1 Hz, *J* = 6.6 Hz), 2.38 (3H, s), OH signal not observed; **^{13}C NMR** (125 MHz, $CDCl_3$): δ 155.5, 145.7, 145.6, 145.5, 135.0, 131.0, 129.7, 128.8, 128.1, 125.1, 124.5, 123.3, 119.3, 116.1, 115.4, 21.6; **LRMS** (+ESI): *m/z* 443/445 (58/48, $[M+H]^+$), 465/467 (100/96, $[M+Na]^+$). **IR** (neat, cm^{-1}): $\tilde{\nu}$ 3370, 1595, 1386, 1175, 1160, 588.

3,5-bis(4-methoxyphenyl)-1H-pyrrolo[2,3-b]pyridine (8a). This compound was prepared according to **general procedure E**. The residue was purified using flash chromatography (hexane/ethyl acetate 3:1 → 1:1) to give the product as a yellow solid (95% yield). m.p. 193-194 °C; R_f (hexane/ethyl acetate 1:1): 0.35; **^{1}H NMR** (300 MHz, $CDCl_3$): δ 11.50 (1H, s), 8.53 (1H, s), 8.37 (1H, d, *J* = 1.6 Hz), 7.59-7.51 (5H, m), 7.03 (4H, d, *J* = 8.6 Hz), 3.87 (6H, s); **^{13}C NMR** (75 MHz, $CDCl_3$): δ 159.4, 158.6, 147.3, 140.2, 131.6, 129.9, 128.6, 128.5, 127.6, 127.2, 123.0, 119.8, 116.7, 114.6 (two overlapping signals), 55.5 (two overlapping signals); **LRMS** (+ESI): *m/z* 331 (100, $[M+H]^+$). **IR** (neat, cm^{-1}): $\tilde{\nu}$ 3115, 3031, 2835, 1500, 1241, 1209, 1027, 831.

3,5-bis(4-methoxyphenyl)-1*H*-indole (8b). This compound was prepared according to **general procedure E**. The residue was purified using flash chromatography (hexane/ethyl acetate 3:1 →

1:1) to give the product as a yellow solid (95% yield). m.p. 153–154 °C; R_f (hexane/ethyl acetate 1:1): 0.35; **^{1}H NMR** (400 MHz, acetone-*d*): δ 10.39 (1H, bs), 8.03 (1H, t, J = 1.0 Hz), 7.67 (2H, dd, J = 2.2 Hz, J = 6.6 Hz), 7.61 (2H, dd, J = 2.2 Hz, J = 6.6 Hz), 7.53-7.51 (2H, m), 7.42 (1H, dd, J = 1.8 Hz, J = 8.4 Hz), 7.04 (1H, d, J = 2.2 Hz), 7.02 (2H, t, J = 2.5 Hz), 7.00 (1H, d, J = 2.2 Hz), 3.84 (3H, s), 3.83 (3H, s); **^{13}C NMR** (100 MHz, acetone-*d*): δ 159.6, 159.0, 137.4, 136.2, 133.7, 129.5, 129.1, 128.9, 127.3, 123.6, 122.0, 118.1, 117.9, 115.1, 115.0, 112.9, 55.6, 55.5; **LRMS** (-ESI): *m/z* 328 (100, $[M - H]^-$). **IR** (neat, cm^{-1}): $\tilde{\nu}$ 3401, 2953, 2834, 1503, 1273, 837.

3,5-bis(4-methoxyphenyl)-1*H*-indazole (8c). This compound was prepared according to **general procedure E**. The residue was purified by flash chromatography (hexane/ethyl acetate 3:1 → 1:1) to give the product as a pale yellow solid (91% yield). m.p. 180-181 °C; R_f (hexane/ethyl acetate 2:1): 0.50; **^{1}H NMR** (500 MHz, DMSO-*d*): δ 13.13 (1H, s), 8.12 (1H, s), 7.98 (2H, d, J = 8.7 Hz), 7.66 (2H, d, J = 8.6 Hz), 7.63 (2H, d, J = 5.9 Hz), 7.10 (2H, d, J = 8.7 Hz), 7.03 (2H, d, J = 8.6 Hz), 3.83 (3H, s), 3.80 (3H, s); **^{13}C NMR** (125 MHz, DMSO-*d*): δ 158.9, 158.5, 143.5, 140.7, 133.4, 133.2, 128.2, 128.1, 126.3, 125.6, 120.6, 117.6, 114.3, 114.3, 110.9, 55.1 (two overlapping signals); **LRMS** (+ESI): *m/z* 331 (100, $[M + H]^+$), 353 (40, $[M + Na]^+$). **IR** (neat, cm^{-1}): $\tilde{\nu}$ 3128, 3024, 2906, 1611, 1243, 804.

4-(3-(4-nitrophenyl)-1-tosyl-1*H*-pyrrolo[2,3-*b*]pyridin-5-yl)phenol (8d). This compound was prepared according to **general procedure C** at 110 °C. The residue was purified by flash chromatography (hexane/ethyl acetate 5:1 → 1:1) to give the product as a yellow solid (87% yield). m.p. 253-255 °C; R_f (hexane/ethyl acetate 2:1): 0.40; **^{1}H NMR** (300 MHz, acetone-d_6): δ 8.65 (1H, s), 8.44 (1H, s), 8.35 (3H, d, J = 7.8 Hz), 8.20-8.15 (4H, m), 7.58 (2H, d, J = 7.9 Hz), 7.44 (2H, d, J = 7.9 Hz), 6.97 (2H, d, J = 8.0 Hz), 2.38 (3H, s); **^{13}C NMR** (75 MHz, acetone-d_6): δ 158.5, 147.8, 147.3, 146.9, 144.9, 140.5, 136.1, 134.2, 130.8, 130.0, 129.6, 129.2, 129.1, 127.2, 126.5, 125.0, 121.4, 118.9, 116.8, 21.5; **LRMS** (+ESI): *m/z* 508 (100, $[M+Na]^+$), 486 (43, $[M+H]^+$). **IR** (neat,

cm^{-1}): $\tilde{\nu}$ 3132, 1594, 1517, 1232, 581.

4-(3-(1*H*-indol-5-yl)-1-tosyl-1*H*-pyrrolo[2,3-*b*]pyridin-5-yl)phenol (8e). This compound was prepared according to **general procedure C** at 110 °C. The residue was purified by flash chromatography (hexane/ethyl acetate 5:1 → 1:1) to give the product as an off-white solid (80% yield). m.p. 142-145 °C; R_f (hexane/ethyl acetate 2:1): 0.45; **^{1}H NMR** (500 MHz, $CDCl_3$): δ 8.62 (1H, d, J = 2.1 Hz), 8.36 (1H, s), 8.22 (1H, d, J = 2.1 Hz), 8.12 (2H, d, J = 8.4 Hz), 7.86-7.85 (2H, m), 7.49 (1H, d, J = 8.4 Hz), 7.42 (3H, dd, J = 2.2 Hz, J = 8.5 Hz), 7.29-7.27 (3H, m), 6.92 (2H, d, J = 8.5 Hz), 6.61 (1H, t, J = 2.2 Hz), 5.46 (1H, br.s), 2.36 (3H, s); **^{13}C NMR** (125 MHz, $CDCl_3$): δ 155.8, 146.9, 145.3, 144.0, 135.7, 135.6, 132.7, 131.2, 129.9, 128.9, 128.6, 128.1, 127.2, 125.3, 124.3, 122.8, 122.5, 122.2, 122.1, 119.9, 116.2, 111.9, 103.1, 21.8; **LRMS** (+ESI): *m/z* 502 (100, $[M+Na]^+$), 518 (25, $[M+K]^+$). **IR** (neat, cm^{-1}): $\tilde{\nu}$ 3410, 1703, 1611, 1318, 1230, 584.

4-(5-(4-hydroxyphenyl)-1-tosyl-1*H*-pyrrolo[2,3-*b*]pyridin-3-yl)benzonitrile (8f). This compound was prepared according to **general procedure C** at 110 °C. The residue was purified by flash chromatography (hexane/ethyl acetate 3:1 → 1:1) to give the product as an off-white solid (89% yield). m.p. 167-169 °C; R_f (hexane/ethyl acetate 3:1): 0.40; **^{1}H NMR** (500 MHz, DMSO-*d*): δ 9.64 (1H, s), 8.66 (1H, d, J = 2.1 Hz), 8.45 (1H, s), 8.37 (1H, d, J = 2.1 Hz), 8.08 (4H, dd, J = 7.2 Hz, J = 8.4 Hz), 7.93 (2H, d, J = 8.3 Hz), 7.60 (2H, dd, J = 2.0 Hz, J = 6.6 Hz), 7.44 (2H, d, J = 8.4 Hz), 6.87 (2H, dd, J = 2.0 Hz, J = 6.6 Hz), 2.34 (3H, s); **^{13}C NMR** (125 MHz, DMSO-*d*): δ 157.5, 145.8, 145.8, 143.6, 137.0, 134.4, 132.9, 132.7, 130.1, 128.6, 128.1, 127.9, 127.7, 126.3, 125.7, 120.1, 118.9, 117.9, 115.9, 109.8, 21.1; **LRMS** (+ESI): *m/z* 488 (100, $[M + Na]^+$), 466 (40, $[M + H]^+$). **IR** (neat, cm^{-1}): $\tilde{\nu}$ 3483, 2226, 1607, 1159, 578.

4-(5-(4-nitrophenyl)-1-tosyl-1*H*-pyrrolo[2,3-*b*]pyridin-3-yl)phenol (8g). This compound was prepared according to **general procedure C** at 110 °C. The residue was purified by flash

chromatography (hexane/ethyl acetate 5:1 → 1:1) to give the product as a pale yellow solid (85% yield). m.p. 136-138 °C; R_f (hexane/ethyl acetate 1:1): 0.50; **^{1}H NMR** (500 MHz, MeOD): δ 8.68 (1H, d, J = 2.2 Hz), 8.38 (1H, d, J = 2.2 Hz), 8.32 (2H, dd, J = 2.1 Hz, J = 6.9 Hz), 8.06 (2H, d, J = 8.5 Hz), 7.94 (1H, s), 7.90 (2H, dd, J = 2.1 Hz, J = 7.0 Hz), 7.53 (2H, dd, J = 2.1 Hz, J = 6.6 Hz), 7.37 (2H, d, J = 8.3 Hz), 6.92 (2H, dd, J = 2.1 Hz, J = 6.6 Hz), 2.37 (3H, s), OH signal not observed; **^{13}C NMR** (125 MHz, MeOD): δ 158.7, 148.8, 148.7, 147.2, 146.0, 144.8, 136.5, 132.1, 130.9, 130.0, 129.5, 129.0, 128.9, 125.2, 124.5, 124.2, 123.4, 122.5, 117.0, 21.5; **LRMS** (+ESI): *m/z* 508 (100, $[M+Na]^+$). **IR** (neat, cm^{-1}): $\tilde{\nu}$ 2919, 1597, 1515, 1346, 587.

4-(5-(1*H*-indol-5-yl)-1-tosyl-1*H*-pyrrolo[2,3-*b*]pyridin-3-yl)phenol (8h). This compound was prepared according to **general procedure C** at 110 °C. The residue was purified by flash chromatography (hexane/ethyl acetate 5:1 → 1:1) to give the product as a pale yellow solid (81% yield). m.p. 136-140 °C; R_f (hexane/ethyl acetate 2:1): 0.45; **^{1}H NMR** (500 MHz, MeOD): δ 8.60 (1H, d, J = 2.1 Hz), 8.25 (1H, d, J = 2.1 Hz), 8.03 (2H, d, J = 8.4 Hz), 7.85 (1H, s), 7.76 (1H, d, J = 1.2 Hz), 7.50 (2H, dd, J = 2.1 Hz, J = 6.6 Hz), 7.46 (1H, d, J = 8.4 Hz), 7.34-7.32 (3H, m), 7.26 (1H, s), 6.92 (2H, dd, J = 2.1 Hz, J = 6.6 Hz), 6.50-6.49 (1H, m), 2.33 (3H, s), NH and OH signals not observed; **^{13}C NMR** (125 MHz, MeOD): δ 158.6, 147.6, 147.0, 145.0, 137.4, 136.6, 136.3, 130.9, 130.3, 130.2, 129.9, 128.8, 128.4, 126.6, 124.9, 123.5, 123.4, 122.6, 122.1, 120.2, 117.0, 112.8, 102.7, 21.5; **LRMS** (+ESI): *m/z* 502 (100, $[M+Na]^+$), 480 (64, $[M+H]^+$). **IR** (neat, cm^{-1}): $\tilde{\nu}$ 3416, 2963, 2926, 1616, 1385, 1172, 589.

4-(3-(4-hydroxyphenyl)-1-tosyl-1*H*-pyrrolo[2,3-*b*]pyridin-5-yl)benzonitrile (8i). This compound was prepared according to **general procedure C** at 110 °C. The residue was purified by flash chromatography (hexane/ethyl acetate 5:1 → 1:1) to give the product as an off-white solid (93% yield). m.p. 203-205 °C; R_f (hexane/ethyl acetate 3:1): 0.40; **^{1}H NMR** (400 MHz, $CDCl_3$): δ 8.67 (1H, d, J = 2.2 Hz), 8.18 (1H, d, J = 2.2 Hz), 8.13 (2H, d, J = 8.4 Hz), 7.85 (1H, s), 7.75 (2H, dd, J

= 2.0 Hz, *J* = 6.6 Hz), 7.66 (2H, dd, *J* = 2.0 Hz, *J* = 6.6 Hz), 7.47 (2H, dd, *J* = 2.1 Hz, *J* = 6.6 Hz), 7.30 (2H, d, *J* = 8.1 Hz), 6.96 (2H, dd, *J* = 2.1 Hz, *J* = 6.6 Hz), 2.38 (3H, s), OH signal not observed; **^{13}C NMR** (100 MHz, $CDCl_3$): δ 155.7, 147.5, 145.6, 144.1, 143.2, 135.4, 133.0, 131.0, 129.9, 129.1, 128.3, 128.2, 127.4, 125.0, 123.3, 122.1, 120.3, 118.8, 116.3, 111.6, 21.8; **LRMS** (+ESI): *m/z* 488 (100, $[M + Na]^+$). **IR** (neat, cm^{-1}): $\tilde{\nu}$ 3510, 3126, 2223, 1609, 1119, 666, 576.

4-(3-(4-(1*H*-tetrazol-5-yl)phenyl)-1-tosyl-1*H*-pyrrolo[2,3-*b*]pyridin-5-yl)phenol (8j). This compound was prepared according to **general procedure D**. The residue was purified using flash chromatography (CH_2Cl_2/MeOH 100:1 → 50:1) to give the product as a white solid (83% yield). m.p. 233-235 °C; R_f (CH_2Cl_2/MeOH 20:1): 0.35; **^{1}H NMR** (500 MHz, MeOD): δ 8.41 (1H, d, *J* = 2.1 Hz), 8.12 (1H, d, *J* = 2.1 Hz), 8.03-8.01 (3H, m), 7.99 (2H, d, *J* = 8.7 Hz), 7.71 (2H, d, *J* = 8.4 Hz), 7.32 (2H, dd, *J* = 2.0 Hz, *J* = 6.6 Hz), 7.27 (2H, d, *J* = 8.2 Hz), 6.81 (2H, dd, *J* = 2.0 Hz, *J* = 6.6 Hz), 2.27 (3H, s), NH and OH signals not observed; **^{13}C NMR** (125 MHz, MeOD): δ 158.7, 157.3, 147.5, 147.2, 144.7, 136.9, 136.4, 134.6, 130.9, 130.2, 129.5, 129.1, 129.0, 128.8, 127.6, 125.5, 124.3, 122.3, 120.5, 116.9, 21.6; **LRMS** (+ESI): *m/z* 531 (100, $[M+Na]^+$). **IR** (neat, cm^{-1}): $\tilde{\nu}$ 3137, 2921, 2852, 1378, 1164, 582.

4-(5-(4-(1*H*-tetrazol-5-yl)phenyl)-1-tosyl-1*H*-pyrrolo[2,3-*b*]pyridin-3-yl)phenol (8k). This compound was prepared according to **general procedure D**. The residue was purified using flash chromatography (CH_2Cl_2/MeOH 100:1 → 50:1) to give the product as a white solid (81% yield). m.p. 244-245 °C; R_f (CH_2Cl_2/MeOH 20:1): 0.35; **^{1}H NMR** (300 MHz, DMSO-*d*): δ 9.66 (1H, br.s), 8.80 (1H, d, *J* = 1.8 Hz), 8.47 (1H, d, *J* = 1.8 Hz), 8.16-8.01 (7H, m), 7.67 (2H, d, *J* = 8.5 Hz), 7.42 (2H, d, *J* = 8.2 Hz), 6.92 (2H, d, *J* = 8.5 Hz), 2.33 (3H, s), NH signal not observed; **^{13}C NMR** (75 MHz, DMSO-*d*): δ 157.2, 155.1, 146.7, 145.6, 143.7, 140.1, 134.6, 131.0, 130.0, 128.8, 128.3, 127.6, 127.5, 127.4, 123.5, 122.8, 122.5, 121.0, 120.1, 115.9, 21.1; **LRMS** (+ESI): *m/z* 531 (100, $[M+Na]^+$). **IR** (neat, cm^{-1}): $\tilde{\nu}$ 3400, 3102, 2927, 1508, 1310, 577.

4-(3-(4-nitrophenyl)-1*H*-pyrrolo[2,3-*b*]pyridin-5-yl)phenol (9a). This compound was prepared according to **general procedure E**. The residue was purified by flash chromatography (CH_2Cl_2/MeOH 100:1 → 50:1) to give the product as a yellow solid (95% yield). m.p. 306-316 °C; R_f (CH_2Cl_2/MeOH 20:1): 0.50; **^{1}H NMR** (500 MHz, DMSO-*d*): δ 12.33-12.29 (1H, br s), 9.59-9.55 (1H, br s), 8.54 (1H, d, J = 2.1 Hz), 8.47 (1H, d, J = 2.1 Hz), 8.26 (2H, d, J = 1.9 Hz), 8.24 (1H, s), 8.10 (2H, d, J = 1.9 Hz), 7.61 (2H, dd, J = 2.1 Hz, J = 8.6 Hz), 6.90 (2H, dd, J = 2.1 Hz, J = 6.6 Hz; **^{13}C NMR** (125 MHz, DMSO-*d*): δ 156.9, 148.4, 144.5, 142.4, 142.2, 129.8, 129.4, 128.3, 127.5, 126.3, 124.9, 124.3, 117.0, 115.8, 112.5; **LRMS** (+ESI): *m/z* 330 (100, $[M+H]^+$). **IR** (neat, cm^{-1}): $\tilde{\nu}$ 3217, 3173, 3024, 2921, 1591, 1341, 1263, 849.

4-(3-(1*H*-indol-5-yl)-1*H*-pyrrolo[2,3-*b*]pyridin-5-yl)phenol (9b). This compound was prepared according to **general procedure E**. The residue was purified by flash chromatography (CH_2Cl_2/MeOH 100:1 → 50:1) to give the product as a yellow solid (93% yield). m.p. 268-271 °C; R_f (CH_2Cl_2/MeOH 20:1): 0.45; **^{1}H NMR** (500 MHz, MeOD): δ 8.40 (2H, dd, J = 1.9 Hz, J = 10.2 Hz), 7.85 (1H, s), 7.56 (1H, s), 7.49 (3H, d, J = 8.6 Hz), 7.44 (1H, dd, J = 1.3 Hz, J = 8.4 Hz), 7.27 (1H, d, J = 3.0 Hz), 6.92 (2H, d, J = 8.5 Hz), 6.52 (1H, d, J = 3.0 Hz), NH and OH signals not observed; **^{13}C NMR** (125 MHz, MeOD): δ 158.0, 148.9, 142.1, 136.7, 132.1, 131.0, 130.1, 129.4, 127.4, 127.1, 126.1, 123.9, 122.5, 120.6, 119.6, 119.1, 116.9, 112.6, 102.5; **HRMS** (ESI+) calcd for $C_{21}H_{15}N_3O$ $[M + H]^+$ 326.1288, found 326,1288. **IR** (neat, cm^{-1}): $\tilde{\nu}$ 3480, 3243, 2916, 1606, 1262, 1248, 690. **HPLC**: 99.1%, RT: 18.2 mins.

4-(3-(4-(1*H*-tetrazol-5-yl)phenyl)-1*H*-pyrrolo[2,3-*b*]pyridin-5-yl)phenol (9c). This compound was prepared according to **general procedure E**. The residue was purified by flash chromatography (CH_2Cl_2/MeOH 50:1 → 10:1) to give the product as a pale yellow solid (90% yield). m.p. 282-284 °C; R_f (CH_2Cl_2/MeOH 20:1): 0.20; **^{1}H NMR** (400 MHz, DMSO-*d*): δ 12.08

(1H, br s), 9.51 (1H, s), 8.51 (1H, d, J = 2.0 Hz), 8.44 (1H, d, J = 2.0 Hz), 8.11 (2H, d, J = 8.4 Hz), 8.07 (1H, d, J = 2.6 Hz), 8.04 (2H, d, J = 8.4 Hz), 7.60 (2H, d, J = 8.6 Hz), 6.89 (2H, d, J = 8.6 Hz), NH of tetrazole and OH signals not observed; **^{13}C NMR** (100 MHz, DMSO-*d*): δ 156.8, 155.3, 148.3, 141.9, 137.9, 129.6, 129.3, 128.3, 127.5, 126.8, 125.6, 124.8, 121.2, 117.1, 115.8, 113.5; **HRMS** (ESI+) calcd for $C_{20}H_{14}N_6O$ $[M + H]^+$ 355.1302, found 355.1302. **IR** (neat, cm^{-1}): $\tilde{\nu}$ 3477, 3263, 3230, 2919, 1612, 1531, 1326, 1262, 1243, 836. **HPLC**: 96.4%, RT: 17.1 mins.

4-(3-(4-aminophenyl)-1*H*-pyrrolo[2,3-*b*]pyridin-5-yl)phenol (9d). This compound was prepared according to **General procedure G.** The residue was purified by flash chromatography (CH_2Cl_2/MeOH 100:1 → 20:1) to give the product as pale yellow solid (84% yield). m.p. 113-115 °C; R_f (CH_2Cl_2/MeOH 20:1): 0.40; **^{1}H NMR** (500 MHz, DMSO-*d*): δ 9.47 (1H, s), 8.39 (1H, d, J = 1.7 Hz), 7.75 (1H, d, J = 1.7 Hz), 7.47 (2H, d, J = 8.4 Hz), 7.36 (2H, d, J = 8.3 Hz), 6.86 (1H, s), 6.80 (1H, d, J = 8.3 Hz), 6.61 (2H, d, J = 8.4 Hz), 6.09-6.08 (2H, m), OH signal not observed; **^{13}C NMR** (125 MHz, DMSO-*d*): δ 156.2, 148.5, 148.4, 141.8, 129.9, 128.2, 128.1, 127.1, 126.6, 124.4, 123.4, 118.0, 116.3, 115.2, 115.0; **HRMS** (ESI+) calcd for $C_{19}H_{15}N_3O$ $[M + H]^+$ 302.1288, found 302.1290. **IR** (neat, cm^{-1}): $\tilde{\nu}$ 3481, 3444, 3359, 3338, 2918, 1552, 1231, 794. **HPLC**: 96.0%, RT: 14.4 mins.

4-(5-(4-nitrophenyl)-1*H*-pyrrolo[2,3-*b*]pyridin-3-yl)phenol (9e). This compound was prepared according to **general procedure E**. The residue was purified by flash chromatography (CH_2Cl_2/MeOH 100:1 → 50:1) to give the product as a yellow solid (93% yield). m.p. 178-180 °C; R_f (CH_2Cl_2/MeOH 20:1): 0.50; **^{1}H NMR** (400 MHz, DMSO-*d*): δ 11.98 (1H, s), 9.39 (1H, s), 8.68 (1H, d, J = 2.1 Hz), 8.52 (1H, d, J = 2.1 Hz), 8.32 (2H, dd, J = 1.9 Hz, J = 6.9 Hz), 8.11 (2H, dd, J = 1.9 Hz, J = 6.9 Hz), 7.78 (1H, d, J = 2.4 Hz), 7.60 (2H, dd, J = 2.0 Hz, J = 6.6 Hz), 6.87 (2H, dd, J = 2.0 Hz, J = 6.6 Hz; **^{13}C NMR** (100 MHz, DMSO-*d*): δ 155.8, 149.1, 146.2, 145.9, 142.0, 128.0, 127.8, 126.2, 126.1, 125.4, 124.0, 123.7, 117.5, 115.7, 115.4; **HRMS** (ESI+) calcd for $C_{19}H_{13}N_3O_3$

$[M + H]^+$ 332.1030, found 332.1032. **IR** (neat, cm^{-1}): $\tilde{\nu}$ 3404, 3119, 2858, 1593, 1336,1267. **HPLC**: 96.8%, RT: 23.0 mins.

4-(5-(1*H*-indol-5-yl)-1*H*-pyrrolo[2,3-*b*]pyridin-3-yl)phenol (9f). This compound was prepared according to **general procedure E**. The residue was purified by flash chromatography (CH_2Cl_2/MeOH 100:1 → 50:1) to give the product as a yellow solid (94% yield). m.p. 241-244 °C; R_f (CH_2Cl_2/MeOH 20:1): 0.45; **^{1}H NMR** (500 MHz, DMSO-*d*): δ 11.72 (1H, s), 11.13 (1H, s), 9.37 (1H, br s), 8.53 (1H, d, J = 2.1 Hz), 8.32 (1H, d, J = 2.1 Hz), 7.86 (1H, d, J = 1.6 Hz), 7.69 (1H, d, J = 2.4 Hz), 7.57 (2H, dd, J = 2.1 Hz, J = 6.6 Hz), 7.50 (1H, d, J = 3.4 Hz), 7.45 (1H, dd, J = 1.7 Hz, J = 8.4 Hz), 7.38 (1H, t, J = 2.7 Hz), 6.87 (2H, dd, J = 2.1 Hz, J = 6.6 Hz), 6.50 (1H, dt, J = 0.7 Hz, J = 2.7 Hz); **^{13}C NMR** (125 MHz, DMSO-*d*): δ 155.6, 148.0, 142.0, 135.2, 130.2, 130.1, 128.3, 127.6, 126.0, 125.9, 125.1, 122.9, 120.9, 118.4, 117.4, 115.7, 114.7, 111.8, 101.4; **HRMS** (ESI+) calcd for $C_{21}H_{15}N_3O$ $[M + H]^+$ 326.1288, found 326.1288. **IR** (neat, cm^{-1}): $\tilde{\nu}$ 3262, 2917, 1459, 1257, 732. **HPLC**: 96.5%, RT: 18.0 mins.

4-(5-(4-(1*H*-tetrazol-5-yl)phenyl)-1*H*-pyrrolo[2,3-*b*]pyridin-3-yl)phenol (9g). This compound was prepared according to **general procedure E**. The residue was purified by flash chromatography (CH_2Cl_2/MeOH 50:1 → 10:1) to give the product as a pale yellow solid (90% yield). m.p. 301-303 °C; R_f (CH_2Cl_2/MeOH 20:1): 0.20; **^{1}H NMR** (400 MHz, DMSO-*d*): δ 12.06 (1H, s), 8.68 (1H, s), 8.55 (1H, s), 8.19 (2H, d, J = 6.3 Hz), 8.05 (2H, d, J = 6.3 Hz), 7.78 (1H, s), 7.61 (2H, d, J = 6.5 Hz), 6.88 (2H, d, J = 6.5 Hz), NH of tetrazole and OH signals not observed; **^{13}C NMR** (100 MHz, DMSO-*d*): δ 155.8, 148.8, 141.7, 141.5, 127.8, 127.7, 127.6, 127.4, 127.4, 127.3, 125.6, 125.5, 123.4, 117.4, 115.7, 115.2; **HRMS** (ESI+) calcd for $C_{20}H_{14}N_6O$ $[M + H]^+$ 355.1302, found 355.1301. **IR** (neat, cm^{-1}): $\tilde{\nu}$ 3330, 2921, 1455, 829, 518. **HPLC**: 95.8%, RT: 17.1 mins.

4-(5-(4-aminophenyl)-1*H*-pyrrolo[2,3-*b*]pyridin-3-yl)phenol (9h). This compound was prepared according to **General procedure G.** The residue was purified by flash chromatography (CH_2Cl_2/MeOH 100:1 → 40:1) to give the product as a pale yellow solid (70% yield). m.p. 216-220 °C; R_f (CH_2Cl_2/MeOH 20:1): 0.30; **^{1}H NMR** (400 MHz, DMSO-*d*): δ 11.66 (1H, s), 9.34 (1H, s), 8.41 (1H, d, J = 2.1 Hz), 8.19 (1H, d, J = 2.1 Hz), 7.65 (1H, d, J = 2.1 Hz), 7.54 (2H, dd, J = 2.1 Hz, J = 6.6 Hz), 7.40 (2H, dd, J = 1.9 Hz, J = 6.6 Hz), 6.85 (2H, dd, J = 2.1 Hz, J = 6.6 Hz), 6.67 (2H, dd, J = 1.9 Hz, J = 6.6 Hz), 5.15 (2H, s); **^{13}C NMR** (100 MHz, DMSO-*d*): δ 155.6, 147.9, 147.8, 141.1, 129.2, 127.6, 127.5, 126.4, 125.9, 123.8, 122.8, 117.4, 115.7, 114.6, 114.4; **HRMS** (ESI+) calcd for $C_{19}H_{15}N_3O$ $[M + H]^+$ 302.1288, found 302.1288. **IR** (neat, cm^{-1}): $\tilde{\nu}$ 3351, 3234, 3024, 2870, 1610, 1542, 1478, 1260, 821, 530. **HPLC**: >99.9%, RT: 13.7 mins.

***N*-(4-(3-(4-hydroxyphenyl)-1*H*-pyrrolo[2,3-*b*]pyridin-5-yl)phenyl)acetamide (10a)**. To a solution of 4-(5-(4-aminophenyl)-1H-pyrrolo[2,3-b]pyridin-3-yl)phenol (**9h**) (50 mg, 0.17 mmol) in acetic acid (5 ml) was added acetic anhydride (24 µl, 0.25 mmol), and the reaction was heated to 110 °C for 5 h. After completion and cooling, the mixture was neutralized with Na_2CO_3 (aq), and extracted with ethyl acetate (3 x 10 mL), and the combined organic layers were dried ($MgSO_4$) and concentrated *in vacuo*. The residue was purified using flash chromatography (CH_2Cl_2/MeOH 100:1 → 50:1) to give the product as a plae yellow solid (45 mg, 77% yield). m.p. 272-275 °C; R_f (CH_2Cl_2/MeOH 20:1): 0.35; **^{1}H NMR** (300 MHz, DMSO-*d*): δ 11.78 (1H, s), 10.02 (1H, s), 9.42 (1H, s), 8.51 (1H, s), 8.31 (1H, s), 7.69-7.68 (5H, m), 7.56 (2H, d, J = 8.0 Hz), 6.86 (2H, d, J = 8.0 Hz), 2.07 (3H, s); **^{13}C NMR** (75 MHz, dmso-*d*): δ 168.3, 155.7, 148.3, 141.5, 138.4, 133.7, 128.2, 127.7, 127.2, 125.7, 124.8, 123.1, 119.5, 117.4, 115.7, 114.9, 24.0; **HRMS** (ESI+) calcd for $C_{21}H_{17}N_3O_2$ $[M + H]^+$ 344.1394, found 344.1396. **IR** (neat, cm^{-1}): $\tilde{\nu}$ 3317, 3088, 2922, 1523, 1244, 886, 516. **HPLC**: 98.3%, RT: 16.3 mins.

***N*-(4-(3-(4-hydroxyphenyl)-1*H*-pyrrolo[2,3-*b*]pyridin-5-yl)phenyl)methanesulfonamide (10b)**.

To a solution of 4-(5-(4-aminophenyl)-1H-pyrrolo[2,3-b]pyridin-3-yl)phenol (**9h**) (50 mg, 0.17 mmol) in H_2O (5 ml) was added methanesulfonyl chloride (20 µl, 0.25 mmol), and the mixture was stirred at room temperature for 10 h. After completion, the mixture was extracted with ethyl acetate (3 x 10 mL), and the combined organic layers were dried ($MgSO_4$) and concentrated *in vacuo*. The residue was purified using flash chromatography (CH_2Cl_2/MeOH 100:1 → 50:1) to give the product as a pale yellow solid (41 mg, 64% yield). m.p. 192-195 °C; R_f (CH_2Cl_2/MeOH 20:1): 0.30; **^{1}H NMR** (400 MHz, DMSO-*d*): δ 11.83 (1H, d, J = 2.2 Hz), 8.51 (1H, d, J = 2.1 Hz), 8.32 (1H, d, J = 2.1 Hz), 7.74 (1H, s), 7.72 (2H, d, J = 1.6 Hz), 7.56 (2H, d, J = 8.7 Hz), 7.31 (2H, d, J = 8.7 Hz), 6.85 (2H, d, J = 8.7 Hz), 5.76 (1H, s), 3.01 (3H, s), OH signal not observed; **^{13}C NMR** (100 MHz, DMSO-*d*): δ 156.1, 148.8, 142.0, 137.9, 135.1, 128.4, 128.1, 126.1, 125.5, 123.6, 120.8, 117.8, 116.2, 115.3, 109.0, 55.4; **HRMS** (ESI+) calcd for $C_{20}H_{17}N_3O_3S$ $[M + H]^+$ 380.1063, found 380.1067. **IR** (neat, cm^{-1}): $\tilde{\nu}$ 3401, 2920, 2893, 1610, 1520, 1152. **HPLC**: 95.9%, RT: 17.5 mins.

1-(4-(3-(4-hydroxyphenyl)-1*H*-pyrrolo[2,3-*b*]pyridin-5-yl)phenyl)urea (10c). To a mixture of 4-(5-(4-aminophenyl)-1H-pyrrolo[2,3-b]pyridin-3-yl)phenol (**9h**) (50 mg, 0.17 mmol), citric acid (326 mg, 1.70 mmol), mannitol (310 mg, 1.70 mmol) and urea (153 mg, 2.55 mmol) were added I_2 (4.3 mg, 0.017 mmol), and the reaction was heated to 80 °C for 6 h. After completion and cooling, water (10 ml) was added and extracted with ethyl acetate (3 x 10 mL), and the combined organic layers were dried ($MgSO_4$) and concentrated *in vacuo*. The residue was purified using flash chromatography (CH_2Cl_2/MeOH 50:1 → 10:1) to give the product as a pale yellow solid (41 mg, 70% yield). m.p. 236-239 °C; R_f (CH_2Cl_2/MeOH 20:1): 0.25; **^{1}H NMR** (500 MHz, DMSO-*d*): δ 11.75 (1H, s), 9.37 (1H, s), 8.66 (1H, s), 8.49 (1H, d, J = 2.0 Hz), 8.28 (1H, d, J = 2.0 Hz), 7.69 (1H, d, J = 1.4 Hz), 7.61 (2H, d, J = 8.6 Hz), 7.56 (2H, d, J = 8.5 Hz), 7.51 (2H, d, J = 8.6 Hz), 6.86 (2H, d, J = 8.6 Hz), 5.87 (2H, s); **^{13}C NMR** (125 MHz, DMSO-*d*): δ 156.1, 155.8, 148.3, 141.5, 139.8, 131.9, 128.5, 127.8, 127.3, 125.9, 124.7, 123.1, 118.3, 117.5, 115.8, 114.9; **HRMS** (ESI+) calcd for $C_{20}H_{16}N_4O_2$ $[M + H]^+$ 345.1346, found 345.1345. **IR** (neat, cm^{-1}): $\tilde{\nu}$ 2954, 2921, 2852,

1535, 1242, 813. **HPLC**: >98.3%, RT: 13.3 mins.

5-bromo-1-tosyl-1*H*-pyrrolo[2,3-*b*]pyridine (11). This compound was prepared according to **general procedure A**. The residue was purified using flash chromatography (hexane/ethyl acetate 20:1 → 10:1) to give the product as a white solid (90% yield). m.p. 140-141 °C; R_f (hexane/ethyl acetate 12:1): 0.50; **^{1}H NMR** (300 MHz, $CDCl_3$): δ 8.41 (1H, d, J = 2.1 Hz), 8.05 (2H, d, J = 8.2 Hz), 7.87 (1H, d, J = 2.1 Hz), 7.73 (1H, d, J = 4.0 Hz), 7.23 (2H, d, J = 8.2Hz), 6.51 (1H, d, J = 4.0 Hz), 2.29 (3H, s); **^{13}C NMR** (75 MHz, $CDCl_3$): δ 145.3, 145.1, 145.0, 134.8, 131.5, 129.5, 127.8, 127.7, 124.2, 114.9, 104.4, 21.4; **LRMS** (+ESI): *m/z* 373/375 (97/100, $[M + Na]^+$). **IR** (neat, cm^{-1}): $\tilde{\nu}$ 1592, 1438, 1153, 664.

1-tosyl-1*H*-pyrrolo[2,3-*b*]pyridine-5-carboxylic acid (12).[46] To a solution of **11** (1.00 equvi, 500 mg) , $Pd(AcO)_2$ (0.05 equiv, 16 mg), 1,1′-Ferrocenediyl-bis(diphenylphosphine) (dppf) (0.10 equiv, 79 mg) and EtN(*i*-Pr) (5.00 equiv, 1.24 mL) in DMF (0.05 M) was added acetic-formic anhydride (5.00 equiv, 626 mg) which was freshly prepared by treating the Ac_2O (5.00 equiv, 673 μL) with formic acid (5.00 equiv, 251 μL) at 65 °C for 30 min,[65] The resulting mixture was heated to 110 °C for 5 h. After completion, it was cooled to RT and diluted by ethyl acetate (30 mL) and quenched with 20% KOH (10 mL) to make pH = 9, the aqueous layer was collected and acidified by con. HCl to adjust pH 4~6, and the corresponding acid was precipitated and filtered to get the desired product without further purification. 83% yield. m.p. 175 °C; R_f (hexane/ethyl acetate 1:1): 0.25; **^{1}H NMR** (300 MHz, DMSO-*d*): δ 13.28 (1H, s), 8.88 (1H, d, J = 2.0 Hz), 8.56 (1H, d, J = 2.0 Hz), 8.03-8.00 (3H, m), 7.42 (2H, d, J = 8.2 Hz), 6.93 (1H, d, J = 4.0 Hz), 2.33 (3H, s); **^{13}C NMR** (75 MHz, DMSO-*d*): δ 166.3, 148.2, 145.9 (two overlapping signals), 134.3, 131.6, 130.1, 128.3, 127.6, 122.4, 122.1, 106.5, 21.1; **LRMS** (+ESI): *m/z* 317 (100, $[M + H]^+$). **IR** (neat, cm^{-1}): $\tilde{\nu}$ 3146, 3102, 2854, 1680, 1528, 1192, 669, 589.

4-((*tert*-butyldimethylsilyl)oxy)aniline (13a). This compound was prepared according to **general procedure H**. The residue was purified using flash chromatography (hexane/ethyl acetate 10:1 → 5:1) to give the product as a pale yellow oil (87% yield). R_f (hexane/ethyl acetate 2:1): 0.45; **^{1}H NMR** (300 MHz, DMSO-*d*): δ 6.53 (2H, d, J = 8.7 Hz), 8.46 (2H, d, J = 8.7 Hz), 4.59 (2H, s), 0.93 (9H, s), 0.11 (6H, s); **^{13}C NMR** (75 MHz, DMSO-*d*): δ 145.5, 142.8, 119.9, 114.9, 25.6, 17.8, -4.6; The spectroscopic data matched that reported in the literature[6].

3-((*tert*-butyldimethylsilyl)oxy)aniline (13b). This compound was prepared according to **general procedure H**. The residue was purified using flash chromatography (hexane/ethyl acetate 10:1 → 5:1) to give the product as a pale yellow oil (93% yield). R_f (hexane/ethyl acetate 2:1): 0.45; **^{1}H NMR** (500 MHz, $CDCl_3$): δ 6.99 (1H, t, J = 8.0 Hz), 6.31-6.26 (2H, m), 6.21-6.20 (1H, m), 3.46 (2H, br.s), 0.99 (9H, s), 0.20 (6H, s); **^{13}C NMR** (125 MHz, $CDCl_3$): δ 156.9, 147.8,130.1, 110.7, 108.7, 107.3, 25.9, 18.3, -4.2; The spectroscopic data matched that reported in the literature[66].

***N*-(4-((*tert*-butyldimethylsilyl)oxy)phenyl)-1-tosyl-1*H*-pyrrolo[2,3-*b*]pyridine-5-carboxamide (14a)**. This compound was prepared according to **general procedure I**. The residue was purified by flash chromatography (hexane/ethyl acetate 5:1 → 3:1) to give the product as a white solid (61% yield). m.p. 190-192 °C; R_f (hexane/ethyl acetate 2:1): 0.35; **^{1}H NMR** (300 MHz, $CDCl_3$): δ 8.81 (1H, d, J = 2.1 Hz), 8.26 (1H, d, J = 2.1 Hz), 8.06-8.03 (3H, m), 7.72 (1H, d, J = 4.0 Hz), 7.48 (2H, d, J = 8.8 Hz), 7.26 (2H, d, J = 8.1 Hz), 6.82 (2H, dd, J = 2.1 Hz, 6.7 Hz), 6.55 (1H, d, J = 4.0 Hz), 2.36 (3H, s), 0.98 (9H, s), 0.19 (6H, s); **^{13}C NMR** (75 MHz, $CDCl_3$): δ 164.5, 152.9, 148.3, 145.8, 143.7, 135.1, 131.5, 129.9, 129.1, 128.3, 127.9, 126.7, 122.4, 122.1, 120.6, 105.6, 25.8, 21.8, 18.3, -4.3; **LRMS** (+ESI): *m/z* 544 (100, $[M + Na]^+$). **IR** (neat, cm^{-1}): $\tilde{\nu}$ 3363, 2954, 2855, 1672, 1508, 1155, 997.

***N*-(3-((*tert*-butyldimethylsilyl)oxy)phenyl)-1-tosyl-1*H*-pyrrolo[2,3-*b*]pyridine-5-carboxamide**

(14b). This compound was prepared according to **general procedure I**. The residue was purified by flash chromatography (hexane/ethyl acetate 5:1 → 3:1) to give the product as a white solid (79% yield). m.p. 105-107 °C; R_f (hexane/ethyl acetate 2:1): 0.35; **^{1}H NMR** (300 MHz, $CDCl_3$): δ 8.82 (1H, d, J = 1.7 Hz), 8.62 (1H, s), 8.22 (1H, d, J = 1.7 Hz), 8.06 (2H, d, J = 8.2 Hz), 7.65 (1H, d, J = 4.0 Hz), 7.41-7.39 (1H, m), 7.28-7.25 (3H, m), 7.18 (1H, t, J = 8.0 Hz), 6.67-6.65 (1H, m), 6.46 (1H, d, J = 4.0 Hz), 2.38 (3H, s), 1.00 (9H, s), 0.23 (6H, s); **^{13}C NMR** (75 MHz, $CDCl_3$): δ 164.9, 156.2, 148.0, 145.7, 144.0, 139.1, 134.8, 129.8, 129.6, 128.9, 128.1, 127.5, 126.6, 122.0, 116.4, 113.2, 112.3, 105.5, 25.7, 21.6, 18.2, -4.4; **LRMS** (+ESI): *m/z* 544 (100, $[M + Na]^+$). **IR** (neat, cm^{-1}): $\tilde{\nu}$ 2952, 2929, 2857, 1596, 1374, 1191, 838, 578.

***N*-(4-hydroxyphenyl)-1*H*-pyrrolo[2,3-*b*]pyridine-5-carboxamide (15a)**. This compound was prepared according to **general procedure E,** under these conditions the TBS protecting group was removed as well. The residue was purified using flash chromatography (CH_2Cl_2/MeOH 50:1 → 30:1) to give the product as a pale yellow solid (96% yield). m.p. 295-297 °C; R_f (hexane/ethyl acetate 1:1): 0.20; **^{1}H NMR** (300 MHz, DMSO-*d*): δ 11.94 (1H, s), 10.04 (1H, s), 9.24 (1H, s), 8.81 (1H, s), 8.53 (1H, s), 7.57-7.54(3H, m), 6.75 (2H, d, J = 8.4 Hz), 6.59 (1H, d, J = 3.0 Hz); **^{13}C NMR** (75 MHz, DMSO-*d*): δ 164.7, 153.6, 149.5, 142.7, 130.9, 127.8, 127.6, 122.9, 122.2, 118.7, 115.0, 100.9; **LRMS** (+ESI): *m/z* 276 (100, $[M + Na]^+$). **IR** (neat, cm^{-1}): $\tilde{\nu}$ 3334, 3114, 2863, 1636, 1535, 1235, 752.

***N*-(3-hydroxyphenyl)-1*H*-pyrrolo[2,3-*b*]pyridine-5-carboxamide (15b)**. This compound was prepared according to **general procedure E,** on which condition, TBS protecting group could also be removed at one-pot. The residue was purified using flash chromatography (CH_2Cl_2/MeOH 50:1 → 30:1) to give the product as a pale yellow solid (94% yield). m.p. 290-295 °C; R_f (hexane/ethyl acetate 1:1): 0.20; **^{1}H NMR** (400 MHz, DMSO-*d*): δ 11.95 (1H, s), 10.13 (1H, s), 9.38 (1H, s), 8.80 (1H, d, J = 2.2 Hz), 8.54 (1H, d, J = 1.8 Hz), 7.59 (1H, dd, J = 2.5 Hz, 3.4 Hz), 7.39 (1H, t, J = 2.1

Hz), 7.20-7.17 (1H, m), 7.11 (1H, t, *J* = 8.0 Hz), 6.60 (1H, dd, *J* = 1.8 Hz, 3.4 Hz), 6.50 (1H, ddd, *J* = 1.0 Hz, 2.4 Hz, 8.0 Hz); **^{13}C NMR** (100 MHz, DMSO-*d*): δ 165.7, 158.0, 150.1, 143.3, 140.9, 129.7, 128.5, 128.2, 123.3, 119.1, 111.5, 111.1, 107.9, 101.5; **LRMS** (-ESI): *m/z* 252 (100, $[M - H]^-$). **IR** (neat, cm^{-1}): $\tilde{\nu}$ 3343, 3283, 3135, 2882, 1619, 1597, 1441, 1212, 760.

***N*-(4-hydroxyphenyl)-3-iodo-1*H*-pyrrolo[2,3-*b*]pyridine-5-carboxamide (16a)**. To a solution of **15a** (127 mg, 0.50 mmol) in dry DMF (10 mL) was added KOH (345 mg, 2.50 mmol) under nitrogen atmosphere at RT, after 10 min, a solution of I_2 (152 mg, 0.60 mmol) in DMF (1 mL) was added dropwise, and the resulting mixture was stirred at RT for 2 h. After completion monitored by TLC, the reaction was quenched with saturated $Na_2S_2O_3$ aqueous, and extracted with ethyl acetate (3 x 10 mL), the organic layers were dried ($MgSO_4$) and concentrated *in vacuo*. The residue was purified by flash chromatography (CH_2Cl_2/MeOH 50:1) to give the product as a white solid (163 mg, 86% yield). m.p. 209-211 °C; R_f (CH_2Cl_2/MeOH 50:1): 0.20; **^{1}H NMR** (400 MHz, DMSO-*d*): δ 12.46-12.32 (1H, br.s), 10.17 (1H, s), 9.30-9.21 (1H, br.s), 8.83 (1H, d, *J* = 2.1 Hz), 8.29 (1H, d, *J* = 2.1 Hz), 7.83 (1H, s), 7.55 (2H, dd, *J* = 2.1 Hz, 6.8 Hz), 6.75 (2H, dd, *J* = 2.1 Hz, 6.8 Hz); **^{13}C NMR** (100 MHz, DMSO-*d*): δ 164.1, 153.7, 149.2, 143.9, 132.1, 130.7, 127.7, 123.7, 122.4, 121.1, 115.0, 55.7; **LRMS** (-ESI): *m/z* 378 (100, $[M - H]^-$). **IR** (neat, cm^{-1}): $\tilde{\nu}$ 3276, 3108, 2921, 1534, 1292, 1167.

***N*-(3-hydroxyphenyl)-3-iodo-1*H*-pyrrolo[2,3-*b*]pyridine-5-carboxamide (16b)**. To a solution of **15b** (127 mg, 0.50 mmol) in dry DMF (10 mL) was added KOH (345 mg, 2.50 mmol) under nitrogen atmosphere at RT, after 10 min, a solution of I_2 (152 mg, 0.60 mmol) in DMF (1 mL) was added dropwise, and the resulting mixture was stirred at RT for 2 h. After completion monitored by TLC, the reaction was quenched with saturated $Na_2S_2O_3$ aqueous, and extracted with ethyl acetate (3 x 10 mL), the organic layers were dried ($MgSO_4$) and concentrated *in vacuo*. The residue was purified by flash chromatography (CH_2Cl_2/MeOH 50:1) to give the product as a white solid (152

mg, 80% yield). m.p. 205-208 °C; R_f (CH_2Cl_2/MeOH 50:1): 0.20; **^{1}H NMR** (300 MHz, DMSO-*d*): δ 12.40 (1H, br.s), 10.26 (1H, s), 9.41 (1H, br.s), 8.84 (1H, d, J = 1.8 Hz), 8.30 (1H, d, J = 1.8 Hz), 7.85 (1H, s), 7.39-7.38 (1H, m), 7.20-7.10 (2H, m), 6.52 (1H, d, J = 7.6 Hz); **^{13}C NMR** (75 MHz, DMSO-*d*): δ 164.6, 157.5, 149.3, 144.1, 140.2, 132.2, 129.2, 127.9, 123.6, 121.1, 111.2, 110.8, 107.6, 55.8; **LRMS** (+ESI): *m/z* 402 (100, $[M + Na]^+$). **IR** (neat, cm^{-1}): $\tilde{\nu}$ 3103, 3068, 2981, 2851, 1553, 1272, 773, 683.

***N*,3-bis(4-hydroxyphenyl)-1H-pyrrolo[2,3-b]pyridine-5-carboxamide (17a)**. This compound was prepared according to **general procedure C** at 110 °C. The residue was purified by flash chromatography (CH_2Cl_2/MeOH 50:1→ 10:1) to give the product as a pale yellow solid (65% yield). m.p. 210-212 °C; R_f (CH_2Cl_2/MeOH 20:1): 0.30; **^{1}H NMR** (500 MHz, DMSO-*d*): δ 12.04 (1H, s), 10.11 (1H, s), 9.42 (1H, br.s), 9.25 (1H, br.s), 8.82 (1H, d, J = 2.0 Hz), 8.73 (1H, d, J = 2.0 Hz), 7.78 (1H, s), 7.57 (2H, d, J = 8.6 Hz), 7.53 (2H, d, J = 8.9 Hz), 6.88 (2H, d, J = 8.6 Hz), 6.75 (2H, d, J = 8.9 Hz); **^{13}C NMR** (125 MHz, , DMSO-*d*): δ 164.7, 156.0, 153.6, 150.0, 143.0, 130.7, 127.8, 127.2, 127.0, 125.3, 123.7, 122.9, 122.4, 116.4, 115.7, 115.0; **HRMS** (ESI+) calcd for $C_{20}H_{15}N_3O_3$ $[M + Na]^+$ 368.1004, found 368.1006. **IR** (neat, cm^{-1}): $\tilde{\nu}$ 3334, 3011, 1636, 1535, 1235. **HPLC**: 98.8%, RT: 16.8 mins.

***N*-(3-hydroxyphenyl)-3-(4-hydroxyphenyl)-1*H*-pyrrolo[2,3-b]pyridine-5-carboxamide (17b).** This compound was prepared according to **general procedure C** at 110 °C. The residue was purified by flash chromatography (CH_2Cl_2/MeOH 50:1→ 10:1) to give the product as a pale yellow solid (60% yield). m.p. 197-200 °C; R_f (CH_2Cl_2/MeOH 20:1): 0.30; **^{1}H NMR** (500 MHz, DMSO-*d*): δ 12.04 (1H, s), 10.18 (1H, s), 9.39 (2H, br.s), 8.80 (1H, d, J = 2.0 Hz), 8.71 (1H, d, J = 2.0 Hz), 7.76 (1H, s), 7.56 (2H, ddd, J = 2.0 Hz, 2.9 Hz, 6.6 Hz), 7.34 (1H, t, J = 2.1 Hz), 7.17-7.15 (1H, s), 7.10 (1H, t, J = 8.0 Hz), 6.87 (2H, ddd, J = 2.0 Hz, 2.9 Hz, 6.6 Hz), 6.50-6.48 (1H, m); **^{13}C NMR** (125 MHz, , DMSO-*d*): δ 165.2, 157.5, 156.0, 150.0, 143.1, 140.3, 129.2, 127.9, 127.2, 125.2,

123.7, 122.9, 116.3, 115.8, 115.7, 111.2, 110.7, 107.5; **HRMS** (ESI+) calcd for $C_{20}H_{15}N_3O_3$ [M + Na]$^+$ 368.1005, found 368.1006. **IR** (neat, cm^{-1}): $\tilde{\nu}$ 3214, 2920, 2851, 1609, 1494, 1312. **HPLC**: 97.8%, RT: 17.7 mins.

5-bromo-1H-pyrrolo[2,3-b]pyridine-3-carboxylic acid (18)[67]. To a solution of **4a** (1 g, 5.0 mmol) in dry CH_2Cl_2 (0.1 M) was added $AlCl_3$ (1.67 g, 12.5 mmol) at 0 °C under nitrogen atmosphere. After 10 min, trichloroacetyl chloride (670 μL, 6 mmol) was added dropwise, and the resulting mixture was stirred at RT for 2 h. After completion monitored by TLC, the reaction was quenched with cold water (20 mL), and extracted with CH_2Cl_2 (3 x 10 mL), the organic layers were dried ($MgSO_4$) and concentrated *in vacuo*. The residue was treated with NaOH aqueous (30 mL, 3M) without further purification, and stirred at RT for 3 h, the resulting mixture was added con. HCl dropwise at 0 °C to adjust pH as 4~6, and the resulting precipitate was filtered and washed by water and hexane, dried in *vacuo* to give the product as a pale yellow solid (856 mg, 70% yield over two steps). m.p. 289-290 °C, R_f (CH_2Cl_2/MeOH 50:1): 0.25; **^{1}H NMR** (500 MHz, DMSO-*d*): δ 12.65 (1H, s), 12.40 (1H, s), 8.41 (1H, d, J = 2.8 Hz), 8.39 (1H, d, J = 2.8 Hz), 8.20 (1H, d, J = 3.7 Hz); **^{13}C NMR** (125 MHz, DMSO-*d*): δ 164.9, 147.1, 143.8, 134.2, 130.5, 120.0, 112.8, 106.0; **LRMS** (-ESI): *m/z* 239/241 (100/99, [M - H]$^-$), **IR** (neat, cm^{-1}): $\tilde{\nu}$ 3407, 3119, 2885, 1680, 1528, 1182, 683. The spectroscopic data matched that reported in the literature[8].

5-bromo-*N*-(4-((*tert*-butyldimethylsilyl)oxy)phenyl)-1*H*-pyrrolo[2,3-*b*]pyridine-3-carboxamide (19a). This compound was prepared according to **General Procedure I**. The residue was purified by flash chromatography (CH_2Cl_2/MeOH 100:1 → 50:1) to give the product as a pale yellow solid (70% yield). m.p. 270-272 °C; R_f (CH_2Cl_2/MeOH 20:1): 0.45; **^{1}H NMR** (500 MHz, DMSO-*d*): δ 12.47 (1H, br.s), 9.76 (1H, s), 8.61 (1H, d, J = 2.9 Hz), 8.43 (1H, d, J = 1.7 Hz), 8.38 (1H, d, J = 2.9 Hz), 7.60 (2H, dd, J = 3.2 Hz, 11.3 Hz), 6.83 (2H, ddd, J = 2.6 Hz, 4.2 Hz, 6.8 Hz),

0.96 (9H, s), 0.19 (6H, s); **^{13}C NMR** (125 MHz, DMSO-*d*): δ 161.8, 150.7, 146.8, 143.7, 133.0, 131.1, 130.3, 121.5, 120.4, 120.0, 112.4, 109.1, 25.6, 17.9, -4.5; **LRMS** (+ESI): *m/z* 468/470 (98/100, $[M+Na]^+$). **IR** (neat, cm^{-1}): $\tilde{\nu}$ 2924, 2853, 1614, 1508, 1291.

5-bromo-*N*-(3-((*tert*-butyldimethylsilyl)oxy)phenyl)-1*H*-pyrrolo[2,3-*b*]pyridine-3-carboxamide (19b). This compound was prepared according to **General Procedure I**. The residue was purified by flash chromatography (CH_2Cl_2/MeOH 100:1 → 50:1) to give the product as a pale yellow solid (75% yield). m.p. 234-235 °C; R_f (CH_2Cl_2/MeOH 20:1): 0.45; **^{1}H NMR** (300 MHz, DMSO-*d*): δ 12.52 (1H, s), 9.80 (1H, s), 8.63 (1H, d, J = 2.1 Hz), 8.48 (1H, s), 8.39 (1H, d, J = 2.1 Hz), 7.41-7.40 (1H, m), 7.36 (1H, d, J = 8.2 Hz), 7.19 (1H, t, J = 8.0 Hz), 6.54 (1H, dd, J = 1.4 Hz, 8.0), 0.97 (9H, s), 0.21 (6H, s); **^{13}C NMR** (75 MHz, DMSO-*d*): δ 162.1, 155.2, 146.9, 143.8, 140.5, 131.1, 130.7, 129.4, 120.5, 114.4, 112.9, 112.5, 111.3, 109.0, 25.5, 17.9, -4.5; **LRMS** (+ESI): *m/z* 446 (100, $[M+H]^+$). **IR** (neat, cm^{-1}): $\tilde{\nu}$ 3362, 3091, 2927, 1637, 1536, 837.

***N*-(4-((*tert*-butyldimethylsilyl)oxy)phenyl)-5-(4-hydroxyphenyl)-1*H*-pyrrolo[2,3-*b*]pyridine-3-carboxamide (20a)**. This compound was prepared according to **general procedure C** at 110 °C. The residue was purified by flash chromatography (CH_2Cl_2/MeOH 50:1→ 20:1) to give the product as a pale yellow solid (63% yield). m.p. 274-275 °C; R_f (CH_2Cl_2/MeOH 20:1): 0.35; **^{1}H NMR** (400 MHz, DMSO-*d*): δ 12.24-12.23 (1H, br.s), 9.73 (1H, s), 9.55 (1H, s), 8.60 (1H, d, J = 2.2 Hz), 8.52 (1H, d, J = 2.2 Hz), 8.38 (1H, d, J = 3.0 Hz), 7.62 (2H, dd, J = 2.2 Hz, 6.8 Hz), 7.52 (2H, dd, J = 2.0 Hz, 6.6 Hz), 6.89 (2H, dd, J = 2.0 Hz, 6.6 Hz), 6.83 (2H, dd, J = 2.2 Hz, 6.8 Hz), 0.96 (9H, s), 0.18 (6H, s); **^{13}C NMR** (100 MHz, DMSO-*d*): δ 162.4, 156.9, 150.6, 147.6, 142.3, 133.3, 129.9, 129.4, 129.3, 128.1, 126.4, 121.5, 119.7, 118.7, 115.9, 109.5, 25.6, 17.9, -4.5; **LRMS** (+ESI): *m/z* 482 (100, $[M+Na]^+$). **IR** (neat, cm^{-1}): $\tilde{\nu}$ 3231, 2954, 1508, 1262.

***N*-(3-((*tert*-butyldimethylsilyl)oxy)phenyl)-5-(4-hydroxyphenyl)-1*H*-pyrrolo[2,3-*b*]pyridine-3-carboxamide (20b)**. This compound was prepared according to **general procedure C** at 110 °C. The residue was purified by flash chromatography (CH_2Cl_2/MeOH 50:1→ 20:1) to give the product as a pale yellow solid (61% yield). m.p. 242-244°C; R_f (CH_2Cl_2/MeOH 20:1): 0.35; **^{1}H NMR** (400 MHz, DMSO-*d*): δ 12.29 (1H, s), 9.76 (1H, s), 9.55 (1H, s), 8.59 (1H, d, J = 2.2 Hz), 8.53 (1H, d, J = 2.3 Hz), 8.43 (1H, d, J = 2.9 Hz), 7.53 (2H, d, J = 8.6 Hz), 7.42 (1H, t, J = 2.1 Hz), 7.40-7.38 (1H, m), 7.20 (1H, t, J = 8.1 Hz), 6.90 (2H, d, J = 8.6 Hz), 6.56-6.54 (1H, m), 0.98 (9H, s), 0.23 (6H, s); **^{13}C NMR** (100 MHz, DMSO-*d*): δ 162.6, 156.9, 155.2, 147.6, 142.4, 140.8, 130.0, 129.7, 129.4, 129.3, 128.1, 126.4, 118.7, 115.9, 114.2, 112.9, 111.2, 109.4, 25.6, 17.9, -4.5; **LRMS** (+ESI): *m/z* 482 (100, $[M+Na]^+$). **IR** (neat, cm^{-1}): $\tilde{\nu}$ 3392, 2953, 2851, 1588, 1203, 830.

***N*,5-bis(4-hydroxyphenyl)-1*H*-pyrrolo[2,3-*b*]pyridine-3-carboxamide (21a)**.[68] To a solution of **20a** (50 mg, 0.11 mmol) in THF (5 mL) was added TBAF (1 M in THF) (170 μL, 0.17 mmol) dropwise and stirred at RT for 1 h. The solvent was removed *in vacuo* and the residue was purified by flash chromatography (CH_2Cl_2/MeOH 20:1→ 10:1) to give the product as a pale yellow solid (35 mg, 93% yield). m.p. 225-227 °C; R_f (CH_2Cl_2/MeOH 10:1): 0.30; **^{1}H NMR** (400 MHz, DMSO-*d*): δ 12.21-12.20 (1H, br.s), 9.64 (1H, s), 9.54 (1H, s), 9.17 (1H, s),8.60 (1H, d, J = 2.2 Hz), 8.51 (1H, d, J = 2.2 Hz), 8.38 (1H, d, J = 2.8 Hz), 7.52 (4H, d, J = 8.6 Hz), 6.89 (2H, d, J = 8.6 Hz), 6.74 (2H, d, J = 8.8 Hz); **^{13}C NMR** (100 MHz, DMSO-*d*): δ 162.3, 156.9, 153.2, 147.6, 142.2, 131.0, 129.9, 129.5, 129.1, 128.1, 126.4, 121.9, 118.8, 115.9, 115.0, 109.6; **HRMS** (ESI+) calcd for $C_{20}H_{15}N_3O_3$ $[M + Na]^+$ 368.1006, found 368.1006. **IR** (neat, cm^{-1}): $\tilde{\nu}$ 3090, 2960, 2873, 1511, 820. **HPLC**: 99.7%, RT: 16.3 mins.

***N*-(3-hydroxyphenyl)-5-(4-hydroxyphenyl)-1*H*-pyrrolo[2,3-*b*]pyridine-3-carboxamide (21b)**. To a solution of **20b** (50 mg, 0.11 mmol) in THF (5 mL) was added TBAF (1 M in THF) (170 μL, 0.17 mmol) dropwise and stirred at RT for 1 h. The solvent was removed *in vacuo* and the residue

was purified by flash chromatography (CH_2Cl_2/MeOH 20:1→ 10:1) to give the product as a pale yellow solid (36 mg, 95% yield). m.p. 280-284 °C; R_f (CH_2Cl_2/MeOH 10:1): 0.30; **^{1}H NMR** (400 MHz, DMSO-*d*): δ 12.25 (1H, d, J = 2.5 Hz), 9.70 (1H, s), 9.55 (1H, s), 9.34 (1H, s), 8.60 (1H, d, J = 2.3 Hz), 8.52 (1H, d, J = 2.3 Hz), 8.43 (1H, d, J = 2.9 Hz), 7.52 (2H, dd, J = 2.0 Hz, 6.6 Hz), 7.37 (1H, t, J = 2.0 Hz), 7.15 (dt, 1H, J = 1.1 Hz, 8.0 Hz), 7.10 (1H, t, J = 8.0 Hz), 6.90 (2H, dd, J = 2.0 Hz, 6.6 Hz), 6.48-6.45 (1H, m); **^{13}C NMR** (100 MHz, DMSO-*d*): δ 162.6, 157.5, 157.0, 147.6, 142.4, 140.6, 130.0, 129.6, 129.5, 129.2, 128.1, 126.4, 118.8, 116.0, 110.6, 110.1, 109.5, 107.0; **HRMS** (ESI+) calcd for $C_{20}H_{15}N_3O_3$ $[M + Na]^+$ 368.1006, found 368.1005. **IR** (neat, cm^{-1}): $\tilde{\nu}$ 3393, 3091, 2921, 1639, 1365. **HPLC**: 99.5%, RT: 17.4 mins.

Biology evaluation. All chemicals were obtained from Sigma Aldrich (St. Louis, MO, USA). Primary antibodies against DYRK1A (#8765), DYRK1B (#2703), DYRK2 (#8143) and p38α (#9218), secondary anti-rabbit (#7074) and anti-mouse (#7076) HRP-linked antibodies were obtained from Cell Signaling Technology (Danvers, MA, USA). EGFR (#sc03) and β-actin (#A5441) antibodies were obtained from Santa Cruz Biotechnology (Dallas, TX, USA) and Sigma Aldrich (St. Louis, MO, USA), respectively. CLK1 antibody (#ab209681) was purchased from Abcam (Cambridge, UK). EGF was purchased from Life Technologies (Carlsbad, CA, USA).

Kinase inhibition assay. Active DYRK1A, DYRK1B, DYRK2 and CLK1 (all Life Technologies) were assayed in Tris buffer (50 mM Tris-HCl, pH 7.5) containing 0.1 mM EGTA, 15 mM DTT, MgAc/ATP cocktail (0.5 mM HEPES pH 7.4; 10 mM $Mg(CH_3COO)_2$; 0.1 mM ATP), [γ-^{32}P]-ATP 100 - 300 cpm/pmol and test compounds diluted in deionized water. As substrate, Woodtide (50 μM, Genscript) was used in DYRK1A, DYRK1B and DYRK2 activity assays, and RS repeat peptide [KKGRSRSRSRSRSR] (20 μM, Genscript) was used in CLK1 activity assays. The reaction was initiated with 1 ng/μL DYRK1A or 0.5 ng/μL DYRK1B, DYRK2 and CLK1. The reaction mixture was incubated at 30 °C for 10 min (DYRK1A) or 40 min (DYRK1B, DYRK2, CLK1)

Reaction was stopped by pipetting 10 µL of the reaction mixture onto P81 paper (Reaction Biology) and washing with 0.75% w/v H_3PO_4 and acetone. P81 papers were transferred to sample bags containing Optiphase Supermix scintillation cocktail (Perkin Elmer) and radioactivity (cpm) was measured with MicroBeta Trilux 2 counter (Perkin Elmer). Compounds that inhibited DYRK1A activity by more than 50% at 10 µM were tested in an eight-point serial dilution at a Log_3 scale. Data were normalized to controls (set as 100% activity) and IC_{50} values calculated by non-linear regression analysis using GraphPad Prism 6.0 (GraphPad, La Jolla, CA, USA). IC_{50} values represent mean ± SEM from 3 independent experiments performed in triplicate.

Cell culture. U251 and A172 cell lines were obtained from the European Collection of Cell Cultures (EACC, Salisbury, UK) through Cell Bank Australia in 2014. Cells were cultured in DMEM medium supplemented with 10% FBS and Antibiotic-Antimycotic (both Life Technologies) at 37 ºC and 5% CO_2. Primary glioblastoma cell lines (RN1, JK2, WK1, SJH1) were derived from glioblastoma specimens, characterized as described[54, 55] and cultured in KnockOut DMEM/F-12 basal medium supplemented with StemPro NSC SFM supplement, 2 mM GlutaMAX-ICTS, 20 ng/mL EGF, 10 ng/mL FGF-β and Antibiotic-Antimycotic solution (all Life Technologies) as adherent cells on flasks coated with MatriGel Matrix (BD Falcon). The protocols were approved by the Human Ethics Committee of the University of Sydney (HREC2013/131) and the Human Ethics Committee of the Royal Brisbane & Women's Hospital (RBWH 2004/161). All cell cultures were routinely tested for mycoplasma infection and the cumulative length of culturing did not exceed 10 passages.

Cell viability assay. U251, A172, RN1, WK1 (2 x 10^3 cells/well) and JK2, SJH1 (4 x 10^3 cells/well) were seeded in 96-well plate and treated on the following day with vehicle or test compounds (0.001 - 50 µM) for 3 days (U251, A172, RN1, JK2) or 5 days (WK1, SJH1). 10 µL of Cell-Titer Blue reagent (Promega, WI, USA) was added to each well and incubated at 37 ºC for 4 h.

Fluorescence was measured with Tecan M200 PRO+ microplate reader (Tecan, Switzerland) at 585 nm. Data were normalized to controls (set as 100% viability) and EC_{50} values calculated by non-linear regression analysis using GraphPad Prism 6.0 (GraphPad, La Jolla, CA, USA). EC_{50} values represent mean ± SEM from 3 independent experiments performed in triplicate.

Clonogenic survival. RN1 (2 x 10^3 cells/well) and U251 (0.5 x10^3 cells/well) were seeded onto 6-well plates and treated on the following day with vehicle or test compounds (0.01 - 5 μM). Cells were grown for 12 days, fixed with 50% methanol and stained with Toluidine Blue (Sigma Aldrich). Colonies were counted using the ImageJ software (Colony Area function). Data were normalized to controls (set as 100% survival) and EC_{50} values calculated by non-linear regression analysis using GraphPad Prism 6.0 (GraphPad, La Jolla, CA, USA). EC_{50} values represent mean ± SEM from 3 independent experiments performed in duplicate. One-way ANOVA, followed by Dunnett's multiple comparison test (GraphPad Prism 6.0) was used to determine statistical significance. $P < 0.05$ was considered as significant.

Migration and invasion assays. U251 (1.7 x 10^3 cells/well), A172 (1.5 x 10^3 cells/well) and RN1 (2.0 x 10^3 cells/well) were seeded onto ImageLock 96-well plates (IncuCyte). For RN1 cells, the plates were pre-coated with MatriGel Matrix (BD Falcon). After 24 hours, each well was scratched using the WoundMaker (IncuCyte) and washed with Dulbecco's PBS (Sigma Aldrich). Migration assays were performed in 1% FBS in DMEM (A172, U251) or 0.2% neural supplement in StemPro NSC SFM (RN1) containing test compounds or DMSO (control). For the invasion assays, 45 μL of MatriGel Matrix and 5 μL of 10x inhibitor (or DMSO) were added to each well and allowed to solidify at 37°C for 30 - 60 min. Once the Matrigel Matrix was set, cells were treated with test compounds or DMSO in 1% FBS in DMEM (A172, U251). The plates were imaged over 72 h (IncuCyte) and the relative wound density (RWD, defined as the cumulative increase of wound confluence as a percentage over time) was analyzed with IncuCyte Zoom software. Velocity (μm/h)

was calculated between 0 - 20 h, where the RWD curves were steep and their slopes constant, following the Wound Healing Data analysis (ibidi GmbH, Version 1.2; http://tinyurl.com/gv6ehvo).

Transient DYRK1A knockdown and EGFR degradation asasy. U251 (7 - 9 x10^5 cells/well) were plated on 6-well plates and incubated overnight or until 60 - 70% confluence. Cells were washed with PBS and treated with transfection medium containing 10 nM *si*RNA-DYRK1A (5' – CCGUAAACUUCAUAACAUUtt – 3') or 10 nM *si*RNA-Ctr (both Ambion Silencer Select) diluted in RNAiMAX®, Opti-MEM® and serum free DMEM (all Life Technologies), according to manufacturer's instructions. Cells were incubated in the transfection medium for 12 - 16 h and then starved overnight in serum free DMEM. For the EGFR degradation assay, starved cells were incubated with cycoheximide (2 µg/mL, 2 h) and treated with EGF (100 ng/mL). Cells were lysed at indicated time points with lysis buffer (1 M Tris, 0.5 M EDTA, 5 M NaCl, 1 M $MgCl_2$, Triton X-100, 0.5 M NaF, 10 % v/v glycerol, 1 mM PMSF, 1mM Na_3VO_4) supplemented with protease inhibitor cocktail (Roche), the protein concentration in lysates was determined with the BCA Protein Assay Kit (Life Technologies) and samples were analyzed by Western blotting.

EGFR degradation assay upon drug treatment. U251 (3 x 10^5 cells/well) were seeded onto 6-well plates and starved in serum free DMEM overnight. Starved cells were incubated with test compounds (2.5 µM) or DMSO (control), treated with cycloheximide (30 µg/mL; 1 h) and EGF (100 ng/mL) for indicated time points. Cells were lysed with lysis buffer (as above), protein concentration was determined with the BCA Protein Assay Kit (Life Technologies) and samples were analyzed by Western blotting.

Cellular Thermal Shift Assay. U251 (8 x 10^6 cells/plate) were seeded onto 100 mm Petri dishes and incubated overnight. Cells were treated with test compound (10 µM) or DMSO for 1 h, harvested, washed with PBS and resuspended in PBS containing protease inhibitor cocktail

(Roche). Cell suspensions were divided into 100 μL aliquots in 0.2 mL PCR tubes. Each tube was heated at indicated temperatures (40 – 70 °C) for 3 min using the Veriti thermal cycler (Life Technologies) followed by 3 min cooling at 25 ºC, and then snap-frozen using liquid nitrogen.

For the ITDRF assay, U251 (8 x 10^6 cells/plate) were seeded onto 100 mm Petri dishes and incubated overnight. Cells were treated with test compound (0 - 20 μM) or DMSO for 1 h, harvested, washed with PBS and re-suspended in PBS containing protease inhibitor cocktail (Roche). Cell suspensions were divided into 100 μL aliquots in 0.2 mL PCR tubes and heated at 54 °C for 3 min using the Veriti Thermal Cycler (Life Technologies) followed by 3 min cooling at 25 ºC, and then snap-frozen using liquid nitrogen. The heat-treated cells were lysed by 3 freeze-thaw cycles using liquid nitrogen and 37 ºC water bath. Cell lysates were centrifuged at 15,000 rpm for 20 min at 4 ºC. Clear supernatants were removed, subjected protein quantification using the BCA Protein Assay Kit (Life Technologies, following manufacturer's instruction) and analyzed by Western blotting.

Western blotting. Cell lysates (20 - 60 μg) or CETSA samples (30 μg) were resolved on 8% or 4 - 12% SDS-PAGE gels and transferred onto PVDF membranes (both Life Technologies). Membranes were blocked with 5% (w/v) skim milk or 15% (w/v) BSA in TBST and incubated with primary antibody overnight at 4 ºC. After washing with TBST, membranes were incubated with their respective secondary antibody for 1 h in RT. Detection was performed with Immobilon Western HRP Substrate Luminol-Peroxidase reagent (MerckMillipore) and the ChemiDoc MP System (BioRad).

ACKNOWLEDGEMENTS

This work was supported by the National Health & Medical Research Council of Australia (APP1106145). LM is a Cancer Institute NSW Career Development Fellow (grant reference 15/CDF/1-07), and the study was supported by Cancer Institute NSW and Brain Foundation

Australia. TGJ, BWS and BWD are members of the Brain Cancer Discovery Collaborative, which is supported by the Cure Brain Cancer Foundation.

Corresponding Author Information

*Corresponding authors

Lenka Munoz

School of Medical Sciences

Charles Perkins Centre

The University of Sydney

New South Wales 2006, Australia

email: lenka.munoz@sydney.edu.au

phone: +61 2 9351 2315

fax: +61 2 8627 1606

Michael Kassiou

School of Chemistry

The University of Sydney

New South Wales 2006

Australia

email: michael.kassiou@sydney.edu.au

phone: +61 2 9351 2745

fax: +61 2 9351 3329

Abbreviations

CDK = cyclin-dependent kinase
CETSA = cellular thermal shift assay
CLK = CDC-like kinase
DIPEA = *N,N*-diisopropylethylamine
dppf = 1,1'-ferrocenediyl-bis(diphenylphosphine)
DYRK = dual-specificity tyrosine phosphorylation-regulated kinases
EGFR = epidermal growth factor receptor
GSK = glycogen synthase kinase
HBTU = (2-(1*H*-benzotriazol-1-yl)-1,1,3,3-tetramethyluronium hexafluorophosphate)
ITDRF = isothermal dose-response fingerprint
MAPK = mitogen-activated protein kinase
NIS = *N*-iodosuccinimide.
OTBS = *tert*-butyldimethylsilyl ether
TBAF = *tetra-n*-butylammonium fluoride

Supporting Information

^{1}H and ^{13}C NMR spectra
HPLC chromatograms
Molecular formula strings

References

1. Varjosalo, M.; Keskitalo, S.; Van Drogen, A.; Nurkkala, H.; Vichalkovski, A.; Aebersold, R.; Gstaiger, M. The protein interaction landscape of the human CMGC kinase group. *Cell Rep.* **2013**, *3*, 1306-1320.

2. Loidreau, Y.; Marchand, P.; Dubouilh-Benard, C.; Nourrisson, M.-R.; Duflos, M.; Loaëc, N.; Meijer, L.; Besson, T. Synthesis and biological evaluation of N-aryl-7-methoxybenzo[b]furo[3,2-d]pyrimidin-4-amines and their N-arylbenzo[b]thieno[3,2-d]pyrimidin-4-amine analogues as dual inhibitors of CLK1 and DYRK1A kinases. *Eur. J. Med. Chem.* **2013**, *59*, 283-295.

3. Abbassi, R.; Johns, T. G.; Kassiou, M.; Munoz, L. DYRK1A in neurodegeneration and cancer: molecular basis and clinical implications. *Pharmacol. Ther.* **2015**, *151*, 87-98.

4. Becker, W.; Sippl, W. Activation, regulation, and inhibition of DYRK1A. *FEBS J.* **2011**, *278*, 246-256.

5. Tejedor, F. J.; Hämmerle, B. MNB/DYRK1A as a multiple regulator of neuronal development. *FEBS J.* **2011**, *278*, 223-235.

6. Smith, B.; Medda, F.; Gokhale, V.; Dunckley, T.; Hulme, C. Recent advances in the design, synthesis, and biological evaluation of selective DYRK1A inhibitors: a new avenue for a disease modifying treatment of Alzheimer's? *ACS Chem. Neurosci.* **2012**, *3*, 857-872.

7. Giraud, F.; Alves, G.; Debiton, E.; Nauton, L.; Théry, V.; Durieu, E.; Ferandin, Y.; Lozach, O.; Meijer, L.; Anizon, F.; Pereira, E.; Moreau, P. Synthesis, protein kinase inhibitory potencies, and in vitro antiproliferative activities of meridianin derivatives. *J. Med. Chem.* **2011**, *54*, 4474-4489.

8. Debdab, M.; Carreaux, F.; Renault, S.; Soundararajan, M.; Fedorov, O.; Filippakopoulos, P.; Lozach, O.; Babault, L.; Tahtouh, T.; Baratte, B.; Ogawa, Y.; Hagiwara, M.; Eisenreich, A.; Rauch, U.; Knapp, S.; Meijer, L.; Bazureau, J.-P. Leucettines, a class of potent inhibitors of CDC2-like kinases and dual specificity, tyrosine phosphorylation regulated kinases derived from the marine

sponge leucettamine B: modulation of alternative pre-RNA splicing. *J. Med. Chem.* **2011**, *54*, 4172-4186.

9. Bain, J.; Plater, L.; Elliott, M.; Shpiro, N.; Hastie, C. J.; McLauchlan, H.; Klevernic, I.; Arthur, J. S. C.; Alessi, D. R.; Cohen, P. The selectivity of protein kinase inhibitors: a further update. *Biochem. J.* **2007**, *408*, 297-315.

10. Göckler, N.; Jofre, G.; Papadopoulos, C.; Soppa, U.; Tejedor, F. J.; Becker, W. Harmine specifically inhibits protein kinase DYRK1A and interferes with neurite formation. *FEBS J.* **2009**, *276*, 6324-6337.

11. Grabher, P.; Durieu, E.; Kouloura, E.; Halabalaki, M.; Skaltsounis, L. A.; Meijer, L.; Hamburger, M.; Potterat, O. Library-based discovery of DYRK1A/CLK1 inhibitors from natural product extracts. *Planta Med.* **2012**, *78*, 951-956.

12. Ogawa, Y.; Nonaka, Y.; Goto, T.; Ohnishi, E.; Hiramatsu, T.; Kii, I.; Yoshida, M.; Ikura, T.; Onogi, H.; Shibuya, H.; Hosoya, T.; Ito, N.; Hagiwara, M. Development of a novel selective inhibitor of the Down syndrome-related kinase Dyrk1A. *Nat. Commun.* **2010**, *1*, 86.

13. Gourdain, S.; Dairou, J.; Denhez, C.; Bui, L. C.; Rodrigues-Lima, F.; Janel, N.; Delabar, J. M.; Cariou, K.; Dodd, R. H. Development of DANDYs, new 3,5-diaryl-7-azaindoles demonstrating potent DYRK1A kinase inhibitory activity. *J. Med. Chem.* **2013**, *56*, 9569-9585.

14. Muraki, M.; Ohkawara, B.; Hosoya, T.; Onogi, H.; Koizumi, J.; Koizumi, T.; Sumi, K.; Yomoda, J.-i.; Murray, M. V.; Kimura, H.; Furuichi, K.; Shibuya, H.; Krainer, A. R.; Suzuki, M.; Hagiwara, M. Manipulation of Alternative Splicing by a Newly Developed Inhibitor of Clks. *J. Biol. Chem.* **2004**, *279*, 24246-24254.

15. Mott, B. T.; Tanega, C.; Shen, M.; Maloney, D. J.; Shinn, P.; Leister, W.; Marugan, J. J.; Inglese, J.; Austin, C. P.; Misteli, T.; Auld, D. S.; Thomas, C. J. Evaluation of substituted 6-arylquinazolin-4-amines as potent and selective inhibitors of cdc2-like kinases (Clk). *Biorg. Med. Chem. Lett.* **2009**, *19*, 6700-6705.

16. Kii, I.; Sumida, Y.; Goto, T.; Sonamoto, R.; Okuno, Y.; Yoshida, S.; Kato-Sumida, T.; Koike, Y.; Abe, M.; Nonaka, Y.; Ikura, T.; Ito, N.; Shibuya, H.; Hosoya, T.; Hagiwara, M. Selective inhibition of the kinase DYRK1A by targeting its folding process. *Nat. Commun.* **2016**, *7*, 11391.

17. Falke, H.; Chaikuad, A.; Becker, A.; Loaëc, N.; Lozach, O.; Abu Jhaisha, S.; Becker, W.; Jones, P. G.; Preu, L.; Baumann, K.; Knapp, S.; Meijer, L.; Kunick, C. 10-Iodo-11H-indolo[3,2-c]quinoline-6-carboxylic acids are selective inhibitors of DYRK1A. *J. Med. Chem.* **2015**, *58*, 3131-3143.

18. Chaikuad, A.; Diharce, J.; Schröder, M.; Foucourt, A.; Leblond, B.; Casagrande, A.-S.; Désiré, L.; Bonnet, P.; Knapp, S.; Besson, T. An unusual binding model of the methyl 9-anilinothiazolo[5,4-f] quinazoline-2-carbimidates (EHT 1610 and EHT 5372) confers high selectivity for dual-specificity tyrosine phosphorylation-regulated kinases. *J. Med. Chem.* **2016**, *59*, 10315–10321.

19. Malinge, S.; Bliss-Moreau, M.; Kirsammer, G.; Diebold, L.; Chlon, T.; Gurbuxani, S.; Crispino, J. D. Increased dosage of the chromosome 21 ortholog Dyrk1a promotes megakaryoblastic leukemia in a murine model of Down syndrome. *J. Clin. Invest.* **2012**, *122*, 948-962.

20. Boichuk, S.; Parry, J. A.; Makielski, K. R.; Litovchick, L.; Baron, J. L.; Zewe, J. P.; Wozniak, A.; Mehalek, K. R.; Korzeniewski, N.; Seneviratne, D. S.; Schöffski, P.; Debiec-Rychter, M.; DeCaprio, J. A.; Duensing, A. The DREAM complex mediates GIST cell quiescence and is a novel therapeutic target to enhance Imatinib-induced apoptosis. *Cancer Res.* **2013**, *73*, 5120-5129.

21. Chang, H.-S.; Lin, C.-H.; Yang, C.-H.; Yen, M.-S.; Lai, C.-R.; Chen, Y.-R.; Liang, Y.-J.; Yu, W. C. Y. Increased expression of DYRK1a in HPV16 immortalized Keratinocytes enable evasion of apoptosis. *Int. J. Cancer* **2007**, *120*, 2377-2385.

22. Chen, J.-Y.; Lin, J.-R.; Feng-Chiao, T.; Meyer, T. Dosage of Dyrk1A shifts cells within a p21-cyclin D1 signalling map to control the decision to enter the cell cycle. *Mol. Cell* **2013**, *52*, 87-100.

23. Litovchick, L.; Florens, L. A.; Swanson, S. K.; Washburn, M. P.; DeCaprio, J. A. DYRK1A protein kinase promotes quiescence and senescence through DREAM complex assembly. *Genes Dev.* **2011**, *25*, 801-813.

24. Di Vona, C.; Bezdan, D.; Islam, Abul B. M. M. K.; Salichs, E.; López-Bigas, N.; Ossowski, S.; de la Luna, S. Chromatin-wide profiling of DYRK1A reveals a role as a gene-specific RNA polymerase II CTD kinase. *Mol. Cell* **2015**, *57*, 506-520.

25. Zhou, N.; Yuan, S.; Wang, R.; Zhang, W.; Chen, J. J. Role of dual specificity tyrosine-phosphorylation-regulated kinase 1B (Dyrk1B) in S-phase entry of HPV E7 expressing cells from quiescence. *Oncotarget* **2015**, *6*, 30745–30761.

26. Guo, X.; Wang, X.; Wang, Z.; Banerjee, S.; Yang, J.; Huang, L.; Dixon, J. E. Site-specific proteasome phosphorylation controls cell proliferation and tumorigenesis. *Nat. Cell Biol.* **2016**, *18*, 202-212.

27. Pozo, N.; Zahonero, C.; Fernández, P.; Liñares, J. M.; Ayuso, A.; Hagiwara, M.; Pérez, A.; Ricoy, J. R.; Hernández-Laín, A.; Sepúlveda, J. M.; Sánchez-Gómez, P. Inhibition of DYRK1A destabilizes EGFR and reduces EGFR-dependent glioblastoma growth. *J. Clin. Invest.* **2013**, *123*, 2475-2487.

28. Ferron, S. R.; Pozo, N.; Laguna, A.; Aranda, S.; Porlan, E.; Moreno, M.; Fillat, C.; de la Luna, S.; Sánchez, P.; Arbonés, M. L.; Fariñas, I. Regulated segregation of kinase Dyrk1A during asymmetric neural stem cell division is critical for EGFR-mediated biased signaling. *Cell Stem Cell* **2010**, *7*, 367-379.

29. Takayama, Y.; May, P.; Anderson, R. G. W.; Herz, J. Low density lipoprotein receptor-related Protein 1 (LRP1) controls endocytosis and c-CBL-mediated ubiquitination of the Platelet-Derived Growth Factor Receptor β (PDGFRβ). *J. Biol. Chem.* **2005**, *280*, 18504-18510.

30. Holgren, C.; Dougherty, U.; Edwin, F.; Cerasi, D.; Taylor, I.; Fichera, A.; Joseph, L.; Bissonnette, M.; Khare, S. Sprouty-2 controls c-Met expression and metastatic potential of colon cancer cells: sprouty/c-Met upregulation in human colonic adenocarcinomas. *Oncogene* **2010**, *29*, 5241-5253.

31. Dominguez, D.; Tsai, Y.-H.; Weatheritt, R.; Wang, Y.; Blencowe, B. J.; Wang, Z. An extensive program of periodic alternative splicing linked to cell cycle progression. *eLife* **2016**, *5*, e10288.

32. Salton, M.; Misteli, T. Small molecule modulators of pre-mRNA splicing in cancer therapy. *Trends Mol. Med.* **2016**, *22*, 28-37.

33. Becker, W. Emerging role of DYRK family protein kinases as regulators of protein stability in cell cycle control. *Cell Cycle* **2012**, *11*, 3389-3394.

34. Gruber, W.; Hutzinger, M.; Elmer, D. P.; Parigger, T.; Sternberg, C.; Cegielkowski, L.; Zaja, M.; Leban, J.; Michel, S.; Hamm, S.; Vitt, D.; Aberger, F. DYRK1B as therapeutic target in Hedgehog/GLI-dependent cancer cells with Smoothened inhibitor resistance. *Oncotarget* **2016**, *7*, 7134-7148.

35. Kettle, J. G.; Ballard, P.; Bardelle, C.; Cockerill, M.; Colclough, N.; Critchlow, S. E.; Debreczeni, J.; Fairley, G.; Fillery, S.; Graham, M. A.; Goodwin, L.; Guichard, S.; Hudson, K.; Ward, R. A.; Whittaker, D. Discovery and optimization of a novel series of Dyrk1B kinase inhibitors to explore a MEK resistance hypothesis. *J. Med. Chem.* **2015**, *58*, 2834-2844.

36. Ewton, D. Z.; Hu, J.; Vilenchik, M.; Deng, X.; Luk, K.-c.; Polonskaia, A.; Hoffman, A. F.; Zipf, K.; Boylan, J. F.; Friedman, E. A. Inactivation of Mirk/Dyrk1b kinase targets quiescent pancreatic cancer cells. *Mol. Cancer Ther.* **2011**, *10*, 2104-2114.

37. Ori-McKenney, Kassandra M.; McKenney, Richard J.; Huang, Hector H.; Li, T.; Meltzer, S.; Jan, Lily Y.; Vale, Ronald D.; Wiita, Arun P.; Jan, Yuh N. Phosphorylation of β-tubulin by the Down syndrome kinase, Minibrain/DYRK1a, regulates microtubule dynamics and dendrite morphogenesis. *Neuron* **2016**, *90*, 551-563.

38. Etienne-Manneville, S. Actin and microtubules in cell motility: which one is in control? *Traffic* **2004**, *5*, 470-477.

39. Schneider, P.; Miguel Bayo-Fina, J.; Singh, R.; Kumar Dhanyamraju, P.; Holz, P.; Baier, A.; Fendrich, V.; Ramaswamy, A.; Baumeister, S.; Martinez, E. D.; Lauth, M. Identification of a novel actin-dependent signal transducing module allows for the targeted degradation of GLI1. *Nat. Commun.* **2015**, *6*, 8023.

40. Hong, S.; Kim, J.; Seo, J. H.; Jung, K. H.; Hong, S.-S.; Hong, S. Design, synthesis, and evaluation of 3,5-disubstituted 7-azaindoles as Trk inhibitors with anticancer and antiangiogenic activities. *J. Med. Chem.* **2012**, *55*, 5337-5349.

41. Goodfellow, V. S.; Loweth, C. J.; Ravula, S. B.; Wiemann, T.; Nguyen, T.; Xu, Y.; Todd, D. E.; Sheppard, D.; Pollack, S.; Polesskaya, O.; Marker, D. F.; Dewhurst, S.; Gelbard, H. A. Discovery, synthesis, and characterization of an orally bioavailable, brain penetrant inhibitor of mixed lineage kinase 3. *J. Med. Chem.* **2013**, *56*, 8032-8048.

42. Himo, F.; Lovell, T.; Hilgraf, R.; Rostovtsev, V. V.; Noodleman, L.; Sharpless, K. B.; Fokin, V. V. Copper(I)-catalyzed synthesis of azoles. DFT study predicts unprecedented reactivity and intermediates. *J. Am. Chem. Soc.* **2005**, *127*, 210-216.

43. Halasz, I.; Biljan, I.; Novak, P.; Meštrović, E.; Plavec, J.; Mali, G.; Smrečki, V.; Vančik, H. Cross-dimerization of nitrosobenzenes in solution and in solid state. *J. Mol. Struct.* **2009**, *918*, 19-25.

44. Kamal, A.; Reddy, J. S.; Bharathi, E. V.; Dastagiri, D. Base-free monosulfonylation of amines using tosyl or mesyl chloride in water. *Tetrahedron Lett.* **2008**, *49*, 348-353.

45. Mahajan, H.; Bhardwaj, M.; Paul, S. Selective synthesis of mono-substituted ureas in low melting citric acid-urea-mannitol mixture. *Org. Prep. Proced. Int.* **2014**, *46*, 463-468.

46. Gadakh, A. V.; Chikanna, D.; Rindhe, S. S.; Karale, B. K. Heteroaryl hydroxycarbonylation: an efficient, robust, practically scalable approach using formyl acetate as the CO Source. *Synth. Commun.* **2012**, *42*, 658-666.

47. Zhang, L.-B.; Hao, X.-Q.; Zhang, S.-K.; Liu, Z.-J.; Zheng, X.-X.; Gong, J.-F.; Niu, J.-L.; Song, M.-P. Cobalt-catalyzed C(sp2)–H alkoxylation of aromatic and olefinic carboxamides. *Angew. Chem. Int. Ed.* **2015**, *54*, 272-275.

48. Zhi-Yong, J.; Yan-Guang, W. A mild, efficient and selective cleavage of aryl tert-butyldimethysilyl ethers using KOH in ethanol. *Chem. Lett.* **2003**, *32*, 568-569.

49. Oakdale, J. S.; Boger, D. L. Total synthesis of Lycogarubin C and Lycogalic acid. *Org. Lett.* **2010**, *12*, 1132-1134.

50. Harrington, P. E.; Bourbeau, M. P.; Fotsch, C.; Frohn, M.; Pickrell, A. J.; Reichelt, A.; Sham, K.; Siegmund, A. C.; Bailis, J. M.; Bush, T.; Escobar, S.; Hickman, D.; Heller, S.; Hsieh, F.; Orf, J. N.; Rong, M.; San Miguel, T.; Tan, H.; Zalameda, L.; Allen, J. G. The optimization of aminooxadiazoles as orally active inhibitors of Cdc7. *Biorg. Med. Chem. Lett.* **2013**, *23*, 6396-6400.

51. Kishore Kumar, G. D.; Natarajan, A. Total synthesis of ovalifoliolatin B, acerogenins A and C. *Tetrahedron Lett.* **2008**, *49*, 2103-2105.

52. Brennan, C. W.; Verhaak, R. G. W.; McKenna, A.; Campos, B.; Noushmehr, H.; Salama, S. R.; Zheng, S.; Chakravarty, D.; Sanborn, J. Z.; Berman, S. H.; Beroukhim, R.; Bernard, B.; Wu, C.-J.; Genovese, G.; Shmulevich, I.; Barnholtz-Sloan, J.; Zou, L.; Vegesna, R.; Shukla, S. A.; Ciriello, G.; Yung, W. K.; Zhang, W.; Sougnez, C.; Mikkelsen, T.; Aldape, K.; Bigner, D. D.; Van Meir, E. G.; Prados, M.; Sloan, A.; Black, K. L.; Eschbacher, J.; Finocchiaro, G.; Friedman, W.; Andrews, D. W.; Guha, A.; Iacocca, M.; O'Neill, B. P.; Foltz, G.; Myers, J.; Weisenberger, D. J.; Penny, R.; Kucherlapati, R.; Perou, C. M.; Hayes, D. N.; Gibbs, R.; Marra, M.; Mills, G. B.; Lander, E.; Spellman, P.; Wilson, R.; Sander, C.; Weinstein, J.; Meyerson, M.; Gabriel, S.; Laird, P. W.; Haussler, D.; Getz, G.; Chin, L. The somatic genomic landscape of glioblastoma. *Cell* **2013**, *155*, 462-477.

53. Pollard, S. M.; Yoshikawa, K.; Clarke, I. D.; Danovi, D.; Stricker, S.; Russell, R.; Bayani, J.; Head, R.; Lee, M.; Bernstein, M.; Squire, J. A.; Smith, A.; Dirks, P. Glioma stem cell lines

expanded in adherent culture have tumor-specific phenotypes and are suitable for chemical and genetic screens. *Cell Stem Cell* **2009**, *4*, 568-580.

54. Day, Bryan W.; Stringer, Brett W.; Al-Ejeh, F.; Ting, Michael J.; Wilson, J.; Ensbey, Kathleen S.; Jamieson, Paul R.; Bruce, Zara C.; Lim, Yi C.; Offenhäuser, C.; Charmsaz, S.; Cooper, Leanne T.; Ellacott, Jennifer K.; Harding, A.; Leveque, L.; Inglis, P.; Allan, S.; Walker, David G.; Lackmann, M.; Osborne, G.; Khanna, Kum K.; Reynolds, Brent A.; Lickliter, Jason D.; Boyd, Andrew W. EphA3 maintains tumorigenicity and is a therapeutic target in glioblastoma multiforme. *Cancer Cell* **2013**, *23*, 238-248.

55. Day, B.; Stringer, B.; Wilson, J.; Jeffree, R.; Jamieson, P.; Ensbey, K.; Bruce, Z.; Inglis, P.; Allan, S.; Winter, C.; Tollesson, G.; Campbell, S.; Lucas, P.; Findlay, W.; Kadrian, D.; Johnson, D.; Robertson, T.; Johns, T.; Bartlett, P.; Osborne, G.; Boyd, A. Glioma surgical aspirate: a viable source of tumor tissue for experimental research. *Cancers (Basel)* **2013**, *5*, 357-371.

56. Molina, D. M.; Jafari, R.; Ignatushchenko, M.; Seki, T.; Larsson, E. A.; Dan, C.; Sreekumar, L.; Cao, Y.; Nordlund, P. Monitoring drug target engagement in cells and tissues using the cellular thermal shift assay. *Science* **2013**, *341*, 84-87.

57. Jafari, R.; Almqvist, H.; Axelsson, H.; Ignatushchenko, M.; Lundbäck, T.; Nordlund, P.; Molina, D. M. The cellular thermal shift assay for evaluating drug target interactions in cells. *Nat. Protocols* **2014**, *9*, 2100-2122.

58. Li, L.; Liu, Y.; Zhang, Q.; Zhou, H.; Zhang, Y.; Yan, B. Comparison of cancer cell survival triggered by microtubule damage after turning Dyrk1B kinase on and off. *ACS Chem. Biol.* **2014**, *9*, 731-742.

59. Becker, W.; Weber, Y.; Wetzel, K.; Eirmbter, K.; Tejedor, F.; Joost, H. Sequence characteristics, subcellular localization, and substrate specificity of DYRK-related kinases, a novel family of dual specificity protein kinases. *J. Biol. Chem.* **1998**, *273*, 25893 - 25902.

60. Esvan, Y. J.; Zeinyeh, W.; Boibessot, T.; Nauton, L.; Théry, V.; Knapp, S.; Chaikuad, A.; Loaëc, N.; Meijer, L.; Anizon, F.; Giraud, F.; Moreau, P. Discovery of pyrido[3,4-g]quinazoline

derivatives as CMGC family protein kinase inhibitors: Design, synthesis, inhibitory potency and X-ray co–crystal structure. *Eur. J. Med. Chem.* **2016**, *118*, 170-177.

61. Munoz, L.; Selig, R.; Yeung, Y.; Peifer, C.; Laufer, S. A. Fluorescence polarisation binding assay to develop inhibitors of inactive p38a mitogen-activated protein kinase. *Anal. Biochem.* **2010**, *401*, 125 - 133.

62. Knight, Z. A.; Shokat, K. M. Features of selective kinase inhibitors. *Chem. Biol.* **2005**, *12*, 621-637.

63. Montanari, S.; Scalvini, L.; Bartolini, M.; Belluti, F.; Gobbi, S.; Andrisano, V.; Ligresti, A.; Di Marzo, V.; Rivara, S.; Mor, M.; Bisi, A.; Rampa, A. Fatty Acid Amide Hydrolase (FAAH), Acetylcholinesterase (AChE), and Butyrylcholinesterase (BuChE): networked targets for the development of carbamates as potential anti-Alzheimer's disease agents. *J. Med. Chem.* **2016**, *59*, 6387-6406.

64. Tasch, B. O. A.; Antovic, D.; Merkul, E.; Müller, T. J. J. One-pot synthesis of camalexins and 3,3′ -biindoles by the Masuda Borylation‐Suzuki arylation (MBSA) sequence. *Eur. J. Org. Chem.* **2013**, *2013*, 4564-4569.

65. Konishi, H.; Muto, T.; Ueda, T.; Yamada, Y.; Yamaguchi, M.; Manabe, K. Imidazole derivatives as accelerators for ruthenium-catalyzed hydroesterification and hydrocarbamoylation of alkenes: extensive ligand screening and mechanistic study. *ChemCatChem* **2015**, *7*, 836-845.

66. Chou, C.-H.; Chen, Y.-Y.; Rajagopal, B.; Tu, H.-C.; Chen, K.-L.; Wang, S.-F.; Liang, C.-F.; Tyan, Y.-C.; Lin, P.-C. Thermally induced denitrogenative annulation for the synthesis of dihydroquinolinimines and chroman-4-imines. *Chem. Asian J.* **2016**, *11*, 757-765.

67. Aronov, A.; Lauffer, D. J.; Li, P.; Tomlinson, R. C. Compositions useful as inhibitors of protein kinases. WO 2003078423 A1, 2005.

68. McKerlie, F.; Rudkin, I. M.; Wynne, G.; Procter, D. J. Evaluation of a new linker system cleaved using samarium(ii) iodide. Application in the solid phase synthesis of carbonyl compounds. *Org. Biomol. Chem.* **2005**, *3*, 2805-2816.

DYRK-CLK inhibition attenuates survival of patient-derived glioblastoma cells

Structural optimization

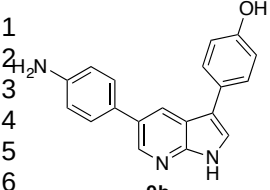

9h

DYRK1A: 43 nM
DYRK1B: 32 nM
DYRK2: 567 nM
CLK1: 34 nM

Cellular target engagement

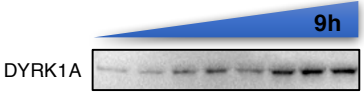

CETSA - ITDRF
DYRK1A: 711 nM

Pharmacology

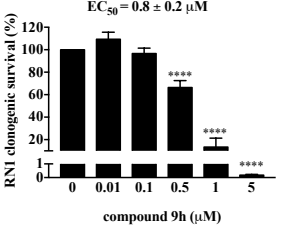

ACS Paragon Plus Environment